Disturbed state concept and non-isothermal shear strength model for unsaturated soils

Tuan A. Pham[1] · Melis Sutman[1]

Abstract

Shear strength of unsaturated soils is an important engineering property that is required for addressing geotechnical problems, the prediction of which remains to be a challenging task for design engineers due to the complex interaction problem. This study presents a new shear strength equation based on the micromechanical model and the disturbed state concept for unsaturated soils. The original point of this study is considering the solid contact area ratio which was neglected in most of the existing equations. Using the proposed model, the non-linear relationship between the matric suction, saturation degree, and the shear strength of unsaturated soils are described. Validation of the shear strength model was verified against the experimental data and several current models on six different types of soils. The results indicate that the proposed model has a good performance in predicting the shear strength of unsaturated soils, and generally is better than other existing models. In response to varying climatic conditions, the analytical model was then extended to consider the effect of temperature on the shear strength of unsaturated soils. The comparison between predicted and measured results was carried out on compacted silt for three different temperatures. The results show that the proposed model is capable of accurately predicting changes in unsaturated shear strength as a function of temperature.

Keywords Unsaturated soil · Shear strength · Effective stress · Matric suction · Disturbed state concept · Temperature · Volume change

Introduction

Geotechnical engineering research in general and unsaturated soil mechanics remain a crucial part of climate change mitigation and adaptation. The temperature increase due to climate change has driven the evaporation as well as changes in subsurface conditions. In these situations, the water amount in soils is constantly changed and soils tend to change from saturated to unsaturated state. As a result, a significant portion of the soil is involved in unsaturated conditions, particularly in the surface soil layers, seasonal areas, soils above the water table, and compacted soils. On the other hand, it is also well-known that the stability of geotechnical structures depends strongly on the accuracy

in predicting the shear strength of soils. In this context, the understanding of shear strength principles of unsaturated soils becomes a topic of interest in addressing geotechnical problems. It is, therefore, crucial to quantify the shear strength of unsaturated soils as well as to be able to respond to the effect of climate change.

The shear strength of unsaturated soils is a highly challenging topic mainly due to their complex multi-phase interaction nature. In practice, the unsaturated shear strength is often predicted by using the two independent stress state variables, named as net normal stress $(\sigma - u_a)$ and matric suction $(u_a - u_w)$. To have a better understanding of unsaturated shear strength, several researchers have efforted to conduct experimental campaigns over the last decades using different test types such as the triaxial test (Blatz and Graham 2003; Houston et al. 2008; Goh et al. 2014; Kim et al. 2018; Satyanaga and Rahardjo 2019), modified triaxial test (Estabragh and Javadi 2008; Patil et al. 2016a, b; Zheng et al. 2020), direct shear test (Hamid and Miller 2009; Nam et al. 2011; Schnellmann et al. 2013; Khaboushan et al. 2018). The experimental results emphasized that the unsaturated shear strength of the soil increases with increasing net normal stress and matric

✉ Tuan A. Pham
ta.pham@hw.ac.uk; anhtuanpham2703@gmail.com

Melis Sutman
m.sutman@hw.ac.uk

1 School of Energy, Geoscience, Infrastructure and Society, Heriot-Watt University, 3.26 William Arrol Building, Edinburgh EH14 4AS, UK

suction, following a nonlinear relationship, yet the level of the nonlinearity depends on the applied net normal stress. The nonlinearity of the shear strength envelope is related to the changes in the degree of saturation of the soil as soil suction changes. Finally, the critical state was also observed and confirmed for unsaturated soils. The above observations should be considered in the development of any analytical models (Pham and Sutman 2021).

Unfortunately, the experimental determination of the shear strength of unsaturated soils is often expensive, time-consuming, and complex. The challenges related to experimental approaches render the numerical methods as a prominent tool in the framework of unsaturated soils. Being a multiphase system, the response of unsaturated soils is based on the grain-scale micromechanical mechanism and therefore shows a particular behaviour compared to other types of materials (Lloret-Cabot et al. 2017). As a result, several different numerical methods were used to study the shear behaviour of unsaturated soils, such as the discrete element method (Jiang et al. 2004; Cai et al. 2020; Kim and Park 2020), finite difference method (Gong et al. 2018), and finite element method (Cho and Lee 2001; Abed and Vermeer 2009). However, the numerical studies related to the shear behaviour of unsaturated soils are still limited due to the complexity of the problem.

In this context, the theoretical framework with mathematical equations also becomes an important tool to predict the shear strength of unsaturated soils. This is particularly true at the preliminary design stage of a project. It is worthy that the general principles associated with the shear strength of saturated soils are often used to apply to unsaturated soils. For engineering purposes, several different equations were proposed to predict the shear strength of unsaturated soils (Bishop et al. 1960; Fredlund et al. 1978; Toll 1990; Vanapalli et al. 1996; Oberg and Sallfors 1997; Khalili and Khabbaz 1998; Miao et al. 2002; Lee et al. 2005; Matsushi and Matsukura 2006; Kayadelen et al. 2007; Zhai et al. 2019). In most cases, the estimated equations are based on the saturated shear strength parameters and the soil–water characteristic curve (SWCC) of the unsaturated soil. Among the existing shear strength equations, most of them are empirical and phenomenological by using fitting parameters. However, the empirical equations are limited to a narrow range of soils employed in the corresponding experiments. Another limitation is that these equations usually require a significant number of input parameters that are not directly available from experimental studies, or they are time-consuming to be identified by laboratory tests. In practice, these methods may produce different results for the same soil sample (Vanapalli and Fredlund 2000; Ye et al. 2010; Patil et al. 2017; Tang et al. 2019; Pham and Sutman 2021; Pham 2022).

It is therefore always desirable to develop a shear strength equation based on the micromechanical theory considering

a multi-phase interaction system for unsaturated soils. In this study, the micromechanical interaction model combined with disturbed state theory is first presented to provide a new equation for predicting the shear strength of unsaturated soils. The proposed model is compared with several existing equations and the experimental results using six published data sets to investigate its validation in the next section. In response to varying climatic conditions, the proposed model is extended to apply to a non-isothermal condition that allows estimating the unsaturated shear strength with temperature changes.

Micromechanical analysis of unsaturated soils

In this section, the micromechanical equilibrium model presented in Pham and Sutman (2021) is refined by the inclusion of a solid contact area ratio by considering the disturbed state concept. In the development of the shear strength model, the following principles are applied:

a) An unsaturated soil can be considered a mixture of three phases, which include solids, pore water, and pore air.
b) The shear strength of unsaturated soils is the result of the interaction between the three phases, and the breaking of the bonds.
c) The models of the individual phases are assembled, using micromechanical equilibrium, to predict the overall shear strength of unsaturated soils.

Therefore, the following analysis starts with the micromechanical stress equilibrium model of three phases to develop a new effective stress equation for unsaturated soils.

Unsaturated effective stress considering the disturbed state

When soil particles are loaded, they tend to reorient and come into contact with one another. The actual example is simplified by postulating a soil made up of homogeneous rigid spheres to better explain the interaction between phases. However, it should be noted that the solution of the analytical model in this paper is established based on the volume relationship and force equilibrium on the total section area without being associated with particle size or particle arrangement. Figure 1a shows the contact of two soil grains in an unsaturated soil. The area of contact between two soil particles is noted as A_c, and the area of the two water membranes embracing the contact area is A_{w1}^m and A_{w2}^m. The load transfer between the two grains is obtained partly through the inter-grain contact area A_c, and partly through the menisci water areas, which can be written as:
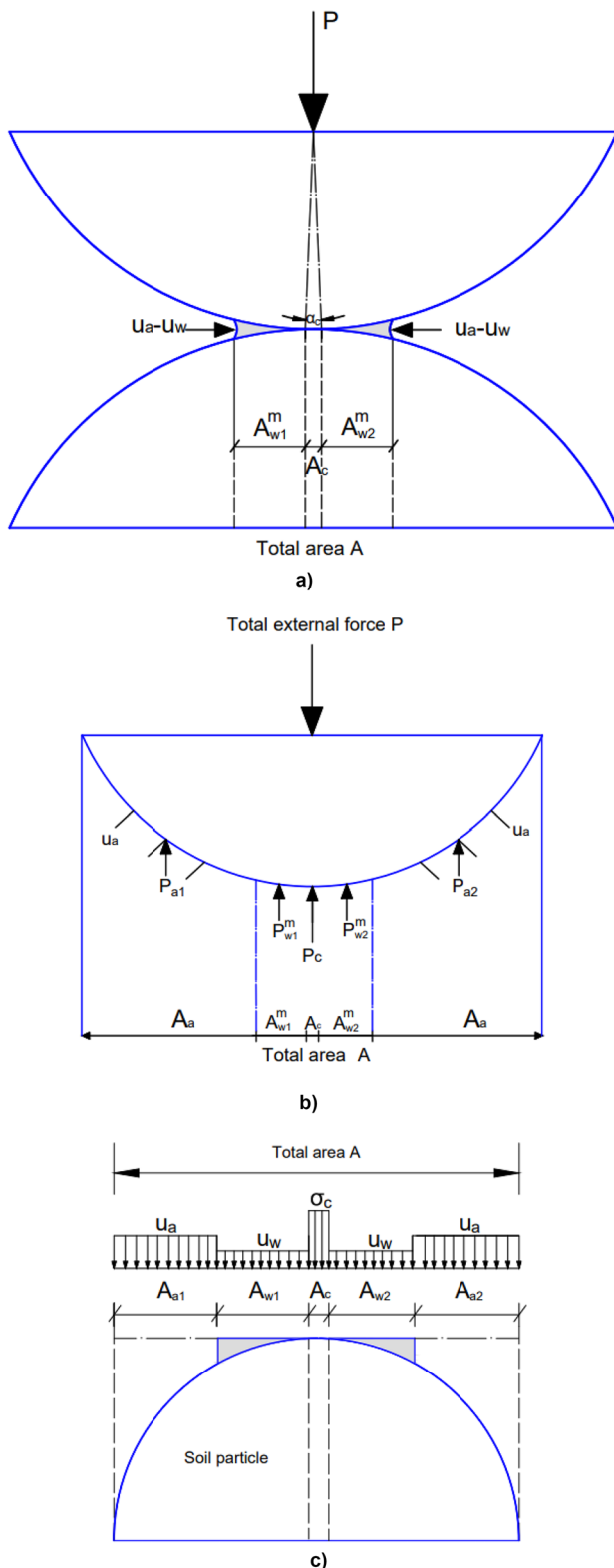
Fig. 1 Stress equilibrium analysis model: **a** representative contact area of unsaturated soils, **b** force interaction analysis, **c** stress distribution in unsaturated soil

$$A_w^m = A_{w1}^m + A_{w2}^m \qquad (1)$$

Most natural soils, on the other hand, have a bimodal structure with a microstructure and a macrostructure. The majority of the macrostructure and the entire microstructure stay saturated when the matric suction range applied to the soil is low. Meanwhile, as suction increases, the saturated soil zone decreases, with only the microstructure saturated (Romero et al. 2001; Rojas 2008; Alonso et al. 2010). As a result, the unsaturated soil is divided into two parts: a saturated portion with "free water" around the soil particles, and an unsaturated fraction with solid particles joined together by water menisci. Because there are certain contact areas between soil particles in free water, it can bear an external load together with the soil skeleton (Karube and Kawai 2001). A water distribution function f is introduced to consider the effect of free water, which was previously overlooked by existing models, and the total water area in an unsaturated soil sample must therefore be:

$$A_w = A_w^f + A_w^m = f . A_w^m \qquad (2)$$

The interaction force system in unsaturated soils is depicted in Fig. 1b. Within the framework of multi-phase continuum mechanics, the equilibrium between internal and external forces for each phase can be described as follows:

$$P = P_c + P_w + P_a \qquad (3)$$

where P is the total external load applied on the unsaturated soil, P_c is the force transferred through the grain contact, P_w is the total force carried by pore water, P_a is the force carried by pore air.

Figure 1c depicts the stress distribution in an unsaturated soil cross-section. It is worth noting that the solid particles make contact with all three phases; therefore, there are two menisci on either side of each contact point. As a result, the force carried by pore water in which the liquid phase reacts, pore air in which the air phase reacts, and solid contact in which the solid phase reacts may be represented as:

$$P_c = \sigma_c . A_c = \sigma' . A \qquad (4)$$

$$P_w = f . (P_{w1}^m + P_{w2}^m) = f . u_w . (A_{w1}^m + A_{w2}^m) \qquad (5)$$

$$P_a = u_a . (A - A_c - f . A_w^m) \qquad (6)$$

$$P = \sigma . A \qquad (7)$$

where P_{w1}^m and P_{w2}^m are the forces carried by water in two menisci surrounding each contact point respectively, u_w is the pore water pressure, u_a is the pore air pressure, A is the

total section area, A_c is the solid contact area between the two soil grains, A_w is the total water area, f is a factor to consider the combined effect of free water and menisci water in unsaturated soils, σ is total stress, σ_c is solid contact stress, σ' is effective stress that represents the equivalent contact stress over the total section area.

In soil mechanics, the term "effective stress" has been adopted in lieu of solid contact stress when calculating the shear strength of the material. This is because soils are a mixture of continuous and discontinuous parts, and the failure state of soils depends on the average stress distribution over the material elements (nonlocal), not at a point (local).

Substituting Eqs. (4) to (7) back into Eq. (3) gives:

$$\sigma.A = \sigma'. A + f.\, u_w.\, A_w^m + u_a.\, (A - A_c - f.\, A_w^m) \tag{8}$$

Dividing both sides of Eq. (8) to the total cross-section area (A) results in:

$$\sigma = \sigma' + f.\, u_w. \frac{A_w^m}{A} + u_a.\, (1 - \frac{A_c}{A} - f.\, \frac{A_w^m}{A}) \tag{9}$$

Rearranging Eq. (9) gives

$$\sigma = \sigma' + f.\, \frac{A_w^m}{A}.\, \left(u_w - u_a \right) + u_a - u_a.\, D \tag{10}$$

where D is the disturbance function, defined as the ratio of solid contact area to total area:

$$D = \frac{A_c}{A} \tag{11}$$

The effective stress equation for unsaturated soils is given by rearranging Eq. (10) as follows:

$$\sigma' = \sigma - u_a + \left(u_a - u_w \right).\, \left(f.\, \frac{A_w^m}{A} + D \right) + u_w.\, D \tag{12}$$

It should be noted that the unsaturated pore water pressure can be calculated by multiplying the pore water pressure at the saturated state with the saturation degree of soils.

Water distribution function in unsaturated soils

Rojas (2008) suggested an equivalent stress model for bimodal structured soil (including micro and macro voids), in which an unsaturated soil is assumed to be divided into two fractions: a saturated fraction, in which soil particles are surrounded by water, and an unsaturated fraction, in which solid particles are linked together by water menisci. Here, a similar technique is utilized, with free water representing the saturated fraction and menisci water representing the unsaturated fraction. The following is the water distribution

function that describes the volume relationship between free water, menisci water, and global water:

$$f = \frac{V_w^f}{V_w^m} + \frac{V_w^m}{V_s}.\, \left[\frac{V}{V_w^m} - \frac{V_w^f}{V_w^m} \right] \tag{13}$$

where V_w^f is free water volume, V_w^m is menisci water volume, and V_s is solid volume.

It should be noted that in the case where soils approach a saturated state, $V_w^f + V_w^m = V_w$, and $f = V/V_w = 1/\theta$. Otherwise, in the case where soils approach very high suction, $V_w^m = V_w$, and $f = 1$. If it is admitted that the value of suction is the same everywhere in the sample, then it can be concluded that all saturated zones are surrounded by menisci of water showing the same radius of curvature as the unsaturated zones. Considering the effective degree of saturation, Eq. (13) can be expressed as:

$$f = 1 + S_e.\, \left[\frac{1}{\theta_e} - 1 \right] \tag{14}$$

where θ_e is normalized volumetric water content, S_e is effective saturation degree.

On the other side, it should be noted that the matric suction is a derivative of the Helmholtz free energy, in which the water distribution function depends on the saturation degree of soils (Lamborn 1986; Aubeny and Lytton 2003; Mun 2005). Equation (14) is in good agreement with the curve of Helmholtz's free energy theory, as illustrated in Fig. 2. The top and lower boundaries of the water distribution function in unsaturated soils are provided by Eq. (14). $f = 1/\theta_e$ for fully saturated soils (zero suction) while $f = 1$ for dry soils (very high soil suction).

Determination of ratio A_w^m/A

If pores are randomly distributed in a homogeneous isotropic material, the areas of water, air, and solids appearing in a cross-section area can be converted to the volumetric distribution of the phases in the following form:

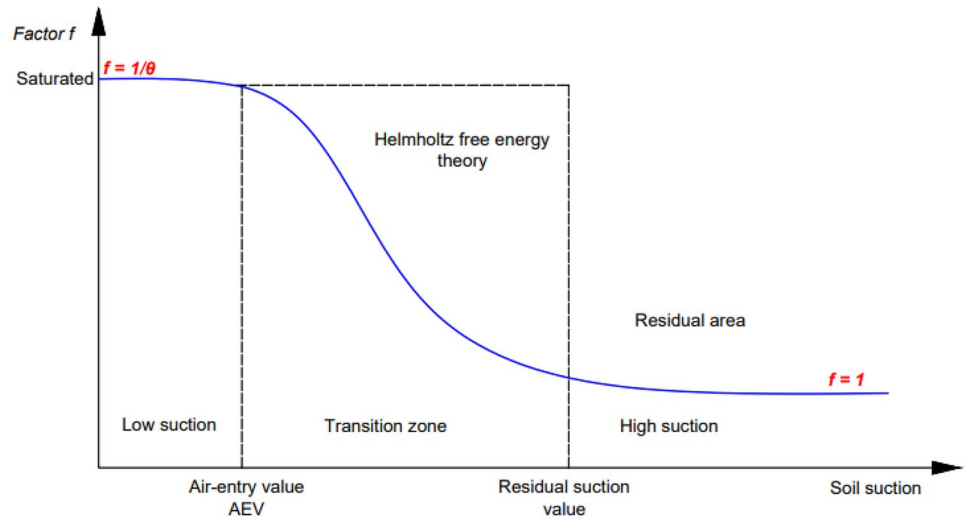$$\theta_e = \frac{A_w^m}{A} = \left(\frac{V_w^m}{V} \right)^{2/3} \tag{15}$$

$$\theta_e = S_e.\, n \tag{16}$$

where n is porosity of soils,

$$S_e = \left(\frac{V_w^m}{V_s} \right)^{2/3} = \frac{S^{2/3} - S_r^{2/3}}{1 - S_r^{2/3}} \tag{17}$$

where S_r = residual degree of saturation.

Fig. 2 SWCC and water distribution function

Disturbance function

The disturbance is the term used to describe the deviation of the current deforming state concerning the initial state (reference state) of the material (Desai and Wang 2003). The disturbance, thus, also represents the variation in the density of soils. Assume that initially, the void volume is higher and that under compressive loading it decreases due to compaction. The change in the void volume of soil can be proportional to the solid-to-solid contact volume, which increases during deformation. The total solid contact volume for a given stage is derived by multiplying the contact area between two solids by the number of interaction points (Fig. 3). The total solid contact volume, therefore, can be expressed as follows:
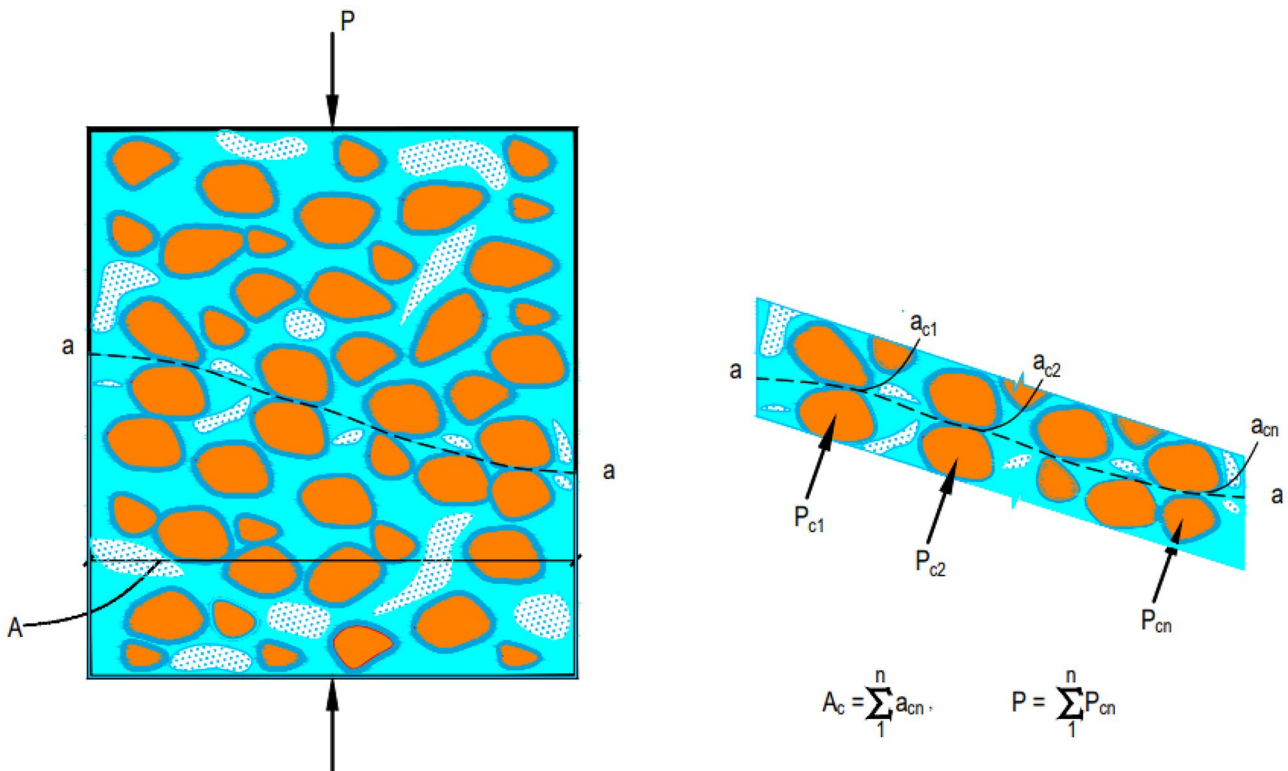

$$A_c = \sum_1^n a_{cn}, \qquad P = \sum_1^n P_{cn}$$

Fig. 3 Unsaturated soils and particle contacts

$$V_c = \sum_{1}^{n} V_{ci} = (\alpha R)^2 . t . n_s \tag{18}$$

where V_c is total solid contact volume, V_{ci} is the contact volume between two solids, α is the contact angle, R is the particle radius, t is the contact thickness, and n_s is the number of contact points. The definition of contact angle is illustrated in Fig. 1a.

On the other side, the following formula serves to convert between two-dimensional and three-dimensional relationships:

$$D = \frac{A_c}{A} = \left(\frac{V_c}{V}\right)^{2/3} \tag{19}$$

The disturbance function thus can be defined by replacing Eq. (18) in Eq. (19) as follows:

$$D = \left(\frac{(\alpha R)^2 . t}{V} . \frac{V}{V_{si}} . \frac{1}{1+e}\right)^{2/3} \tag{20}$$

where V_{si} is the volume of a solid particle ($V_{si} = 4\pi R^3/3$), e is the void ratio of the soil sample.

In this study, the contact angle at the loosest state is assumed to be approximately 10° for sands and 25° for clays, and contact thickness is considered $t = 2R$. Therefore, the approximate solution for the disturbance function is implied as follows:

$$D \approx \frac{0.06}{(1+e)^{2/3}} \text{ for sands} \tag{21}$$

$$D \approx \frac{0.2}{(1+e)^{2/3}} \text{ for clays} \tag{22}$$

On the other hand, if the result of the shear test at a saturated state is available, the disturbance function can be derived empirically. It is possible to calculate the empirical disturbance function as follows:

$$D = 1 - \frac{1}{u_w} . \left(\sigma - \frac{\tau_m - c'}{\tan\varphi'}\right) \tag{23}$$

where u_w is pore-water pressure, τ_m is measured shear stress at a saturated state, c' is the effective cohesion, ϕ' is the friction angle of soils.

Discussion of Terzaghi effective stress equation

Substituting Eqs. (14) and (15) back into Eq. (12) give a general form of effective stress as follows:

$$\sigma' = \sigma - u_a + (u_a - u_w) . \left[\theta_e + S_e.(1 - \theta_e) + D\right] + u_w . D \tag{24}$$

For unsaturated soils, Eq. (24) represents a general form of effective stress. Considering two special cases where soils are completely saturated, and soils are completely dry:

If soils are completely saturated ($u_a = u_w$), Eq. (24) can be revised as:

$$\sigma' = \sigma - u_w(1 - D) \tag{25}$$

If soils are completely dry ($A_w^m = 0$), Eq. (24) can be re-written as:

$$\sigma' = \sigma - u_a(1 - D) \tag{26}$$

On the other side, the Terzaghi effective stress equation is also well-known as follows:

$$\sigma' = \sigma - u_w \tag{27}$$

By comparing Eqs. (25) and (27), it can be observed that the main difference between the proposed equation and Terzaghi's effective stress equation for saturated soils is the term disturbance (D). If the solid contact area is neglected, Eq. (25) becomes an identical one of Terzaghi's effective stress equation. Unlike saturated soils, however, the pore water pressure in unsaturated soils causes both local and non-local actions (Jennings and Burland 1962), which are reflected well in the proposed equation.

Unsaturated shear strength equation

The shear strength constitutive relationship provides a mathematical equation relating the normal and shear components of the stress tensors. To predict the shear strength, the Mohr–Coulomb failure criterion was extended to embrace unsaturated soils by Fredlund et al. (1978). The proposed shear strength equation for unsaturated soils can be written as follows:

$$\tau = c' + (\sigma - u_a) \tan \varphi' + (u_a - u_w) . \left[\theta_e + S_e . (1 - \theta_e) + D\right] \tan \varphi' + u_w . D \tan \varphi' \tag{28}$$

where c' is the effective cohesion, φ' is the friction angle of soils under saturated conditions.

Considering the proposed equation, the soil property function (SPF), which defines the relationship between shear strength and soil suction, is therefore derived as follows:

$$SPF = \left[\theta_e + S_e . (1 - \theta_e) + D\right] \tan \varphi' \tag{29}$$

Alternatively, several researchers preferred to use the term "cohesion intercept" to emphasize the role of matric suction in contributing to the total shear strength of unsaturated soils. The cohesion intercept (c_i) is often defined by:

$$c_i = c' + (u_a - u_w). \left[\theta_e + S_e. (1 - \theta_e) + D\right] tan\, \varphi' \quad (30)$$

Critical shear strength equation

Several critical state shear strength equations have also been proposed for unsaturated soils (Alonso et al. 1990; Wheeler and Sivakumar 1995; Wang et al. 2002; Tarantino 2007; Patil et al. 2017). The proposed equations attempt to describe the shear strength of unsaturated soils under critical state conditions in terms of q-p-r space. A general equation form for incorporating matric suction into the critical state shear strength equation can be written as follows:

$$q = \frac{6c' \cos \varphi'_{cs}}{3 - \sin \varphi'_{cs}} + M(p - u_a) + (u_a - u_w) \\ \cdot \left[\theta_e + S_e.(1 - \theta_e) + D\right]M + u_w. D. M \quad (31)$$

$$p = \frac{1}{3}(\sigma_1 + 2\sigma_3) \quad (32)$$

$$M = \frac{6 \sin \varphi'_{cs}}{3 - \sin \varphi'_{cs}} \quad (33)$$

where M is the slope of the critical state line for saturated soils or critical state stress ratio, p is the net mean stress, q is the deviatoric stress.

Discussion of Bishop's parameter

Bishop et al. (1960) proposed a shear strength equation for unsaturated soils as follows:

$$\tau = c' + \left[(\sigma - u_a) + \chi(u_a - u_w)\right]tan\varphi' \quad (34)$$

where χ is an empirical parameter. The value of χ has a magnitude between 1 and 0. $\chi = 1$ represents the completely saturated condition, and $\chi = 0$ shows a dry state. However, χ depends on many factors such as soil structure, suction, air-entry value, making it difficult to be estimated. By comparing Eqs. (24) and (34), the value of Bishop's parameter χ can be expressed as below:

$$\chi = \theta_e + S_e. (1 - \theta_e) + D \quad (35)$$

In this expression, Bishop's parameter χ depends on several factors such as porosity of soils, volumetric water content, residual degree of saturation, disturbance function, which is in good agreement with previous studies (Rojas 2008; Niu et al. 2021). This expression eliminates the necessity of assuming the parameter χ equal to saturation degree solely.

Review of several existing shear strength equations

Numerous equations have been proposed for describing the shear strength of unsaturated soils, which are subdivided into two main categories: fitting equations and estimation equations. Fitting equations are the ones that can be the best fit for a dataset for the determination of one or more fitting parameters, while estimation equations are the ones based on saturated shear strength parameters and additional information. Some equations either directly or indirectly make use of the properties of the SWCC and others utilize additional information such as soil classification or the shear strength at residual suction conditions. It should be noted that most of the equations are empirical and phenomenological. These equations assume that the shear strength of unsaturated soils can be viewed as an extension of saturated shear strength properties. However, the important difference between existing shear strength equations is in the soil property function (SPF), where a different form of SPF will produce a new shear strength equation.

Considering the characteristics of SPF among existing equations, it can be classified into five main equation groups as follows: (1) shear strength equations with SPF depending on volumetric water content (Lamborn 1986; Aubeny and Lytton 2003), (2) shear strength equations with SPF depending on normalized water content (Vanapalli et al. 1996; Fredlund et al. 1996; Tarantino and Tombolato 2005; Patil et al. 2017), (3) shear strength equations with SPF depending on saturation degree (Oberg and Sallfors 1997; Zhai et al. 2019), (4) shear strength equations with SPF depending on the air-entry value (Khalili and Khabbaz 1998; Miao et al. 2002; Lee et al. 2005; Kayadelen et al. 2007; Satyanaga & Rahardjo 2019), and (5) shear strength equations with SPF depending on residual suction (Rassam and Cook 2002; Naghadeh and Toker 2019). In this study, a representative equation of each group is selected for comparison, and the following section briefly describes the characteristics of the selected shear strength models.

Shear strength equation of Lamborn (1986)

Lamborn (1986) proposed a model for predicting the shear strength of unsaturated soils in which the SPF is assumed to be equal to the volumetric water content (θ). This shear strength equation is expressed as follows:

$$\tau = c' + (\sigma - u_a)tan\, \varphi' + (u_a - u_w)(\theta)tan\, \varphi' \quad (36)$$

Shear strength equation of Vanapalli et al. (1996)

One of the well-known shear strength equations is the model proposed by Vanapalli et al. (1996), where the SPF is assumed to be equal to the normalized volumetric water content or the

so-called effective degree of saturation. The unsaturated shear strength equation is expressed as follows:

$$\tau = c' + (\sigma - u_a)tan\ \varphi' + (u_a - u_w)\left(\frac{\theta - \theta_r}{\theta_s - \theta_r}\right)tan\ \varphi' \quad (37)$$

where θ_r = volumetric water content at residual suction, θ_s = volumetric water content at saturated condition.

Shear strength equation of Oberg and Sallfors (1997)

Oberg and Sallfors (1997) proposed the SPF to be equal to the saturation degree. The expression for this shear strength model is:

$$\tau = c' + (\sigma - u_a)tan\ \varphi' + (u_a - u_w)(S)tan\ \varphi' \quad (38)$$

Shear strength equation of Khalili and Khabbaz (1998)

Khallili and Khabbaz (1998) have extended Bishop's equation by imposing an empirical constant for predicting the shear strength of unsaturated soils. In this approach, the SPF is assumed as a dependent function of the air-entry value (AEV). The shear strength equation is written as follows:

$$\tau = c' + (\sigma - u_a)tan\ \varphi' + (u_a - u_w)\left(\frac{u_a - u_w}{AEV}\right)^{-0.55}tan\ \varphi' \quad (39)$$

Shear strength equation of Naghadeh and Toker (2019)

Naghadeh and Toker (2019) presented a hyperbolic equation for predicting the unsaturated shear strength, in which the SPF depends on the transition suction value. The shear strength equation is expressed as follows:

$$\tau = c' + (\sigma - u_a)tan\ \varphi' + (1 - e^{-(u_a - u_w)/(u_a - u_w)_r}).\ (u_a - u_w)_r.\ tan\ \varphi' \quad (40)$$

where $(u_a - u_w)_r$ is residual suction (or transition suction) that corresponds to residual saturation degree.

Comparison of analytical and experimental results

Soil–water characteristic curve and evaluation criterion

The proposed model is validated against some of the existing shear strength equations and measured data for six different soil types: silty clay, sand, silty soil, clay, expansive soil, and sand-kaolin mixture. It should be noted that Eq. (28) of the proposed model is used to obtain results for comparison in the following sections. To predict the unsaturated shear strength of unsaturated soils, the soil–water characteristic curve (SWCC), which shows the relationship between measured suction and degree of saturation, must be presented. In this study, the SWCC model of Fredlund and Xing (1994) is used to plot the reference curve. This model can be expressed as follows:

$$S = \frac{1}{(ln[2.718 + ((u_a - u_w)/a))^n])^m} \quad (41)$$

where a, m, n are fitting parameters.

It should be noted that the SWCC and shearing tests are performed on different soil specimens which usually do not have the same boundary conditions (e.g., confining pressure). As a result, the initial void ratios of specimens in those two tests may differ. It is worth noting that a difference in void ratios might produce a change in SWCC, affecting the accuracy of shear strength estimation (Ng and Pang 2000; Lee et al. 2005; Krisdani et al. 2008; Dastjerdi et al. 2014; Oh and Lu 2014; Roy and Rajesh 2018; Zhai et al. 2020; Pham 2022). The calibration procedure for SWCC, therefore, must be undertaken based on the real void ratio of shear test samples in order to overcome the uncertainty of SWCC related to the test conditions. Pham and Sutman (2022) proposed a simplified model for predicting SWCC change with initial density. There are three major advantages to this model: (i) it directly correlates the change in suction with the void ratio, (ii) it predicts the influence of volume change on SWCC using the initial void ratio rather than the current void ratio, and (iii) particle shape and pore size are taken into account within the model. As a result, if SWCC calibration is required due to diverse void ratios, it is recommended to choose this model for implementation, the expression of which is as follows:

$$\begin{cases} S_{e_i} = S_{e_0} = \dfrac{1}{ln\left(2.7127 + [(u_a - u_w)_{e_0}/a]^n\right)^m} \\ (u_a - u_w)_{e_i} = (u_a - u_w)_{e_0} \times \sqrt{\dfrac{e_0}{e_i}.\left(\dfrac{1+e_i}{1+e_0}\right)^{1-\delta}} \end{cases} \quad (42)$$

where e_0 is the initial void ratio of soil sample in SWCC test, which is referred to as reference initial void ratio, e_i is the initial void ratio of soil sample in shear test, $(u_a - u_w)_{e_0}$ and $(u_a - u_w)_{e_i}$ are matric suctions corresponding to the initial void ratios of e_0 and e_i, δ is calibrated constant considering the effect of actual particle shape and size. To determine the parameter δ, at least two SWCC test data sets at different void ratios are required. When the data of the SWCC test corresponding to different void ratios is unavailable, δ can be approximated to be between 10 and 15 for sands and silts, between 25 and 35 for clays, and between 45 and 55 for compacted bentonite (Pham and Sutman 2022).

Figure 4 shows an example of the SWCC calibration technique utilizing a measured data source from Habasimbi and Nishimura (2019). Figure 4a shows the compression curve where void ratio versus confining pressure (e-lnσ'). It can be observed that the void ratio of the soil sample decreases with increasing confining pressure. For example, the void ratio reduces from 0.726 to 0.711 as the confining pressure is increased from 20 to 600 kPa. Figure 4b shows the SWCC test results at 20 kPa confining pressure ($e_0 = 0.726$) and calibrated SWCCs at various confining pressures using Eq. (42). It should be emphasized that in Eq. (42), the initial void ratio, $e_0 = 0.726$, is kept constant as a baseline, and then, the calibrated SWCCs were plotted by replacing the arbitrary void ratio corresponding to different confining pressures. As a result, the effect of volume change and confining pressure on the SWCCs may be adequately modeled. If the confining pressure applied during the SWCC test differs from one of the shear tests, the calibrated SWCCs are recommended to be used to estimate the shear strength of unsaturated soil instead of the tested SWCC results (Pham 2022).

The SWCC results of six different soil types, in which the procedure to determine the air-entry value and residual value are illustrated, are presented in Fig. 5. The physical properties of tested soils and input parameters for shear strength equations are summarized in Table 1.

The performance of shear strength models is assessed through the agreement degree of the curve, which represents the difference between the predicted and the measured curves. The agreement degree of the curve is specialized by average relative error (*ARE*), which is defined as the percentage of a discrepancy between the value predicted by the analytical equations and the measured one, according to the following expression:

$$ARE = \frac{1}{N} \sum_{1}^{n} \left| \frac{\tau_{\text{predicted}} - \tau_{\text{measured}}}{\tau_{\text{measured}}} \right| \cdot 100\% \qquad (43)$$

where τ_{measured} is the measured shear strength value of ith data, $\tau_{\text{predicted}}$ is the predicted value of shear strength of ith data, and N is the total number of data points available.

Comparison results for reconstituted silty clay

Cunningham et al. (2003) conducted a series of triaxial compression tests on the reconstituted silty clay, which was made up of 20% pure Speswhite kaolin, 10% London clay, and 70% silica silt, at varied confining pressures. The slurry soil was pre-consolidated to 130 kPa in an isotropic manner. All of the soil samples utilized in this study were reconstituted soils made from a slurry made at 1.5 times the soil's liquid limit. In a 204 mm diameter lever arm oedometer, the slurry was pre-consolidated one-dimensionally to a maximum vertical effective stress of 200 kPa. After that, the sample was

discharged under completely drained conditions to ensure that the initial suction was minimal. The interesting point of these test sets is that an air-circulation system was employed to remove moisture from the base of the triaxial sample, and the suctions are independently measured using a sample-mounted suction probe.

The findings predicted by the proposed model and test data for the suction range of 400 to 1000 kPa are shown in Fig. 6a. When the value *ARE* is just 1.1%, the proposed model exhibits excellent agreement with measured data for four distinct suction levels. In Fig. 6b, a comparison of shear strength equations and measured data with variations in matric suction is shown, with a constant net normal stress of 400 kPa. The shear strength increases with increasing suction, according to both measured and predicted data. The performance of estimation equations, on the other hand, is vastly different. In comparison to other equations, the proposed model has the best agreement with the measured data. The model of Khalili and Khabbaz (1998) with a value *ARE* of 26.1% over-predicts significantly while the models of Lamborn (1986) with a value *ARE* of 50.5% underpredict strongly the unsaturated shear strength. Another finding is that the difference in predicted results between the models of Vanapalli et al. (1996), Oberg and Sallfors (1997), and Naghadeh and Toker (2019) is negligible. This is because the saturation degree of soils, in this case, was relatively high, and the normalized volumetric water contents are approximately equal to the saturation degree. Value *ARE* of these three models is 13.4%, 12.2%, and 11.3%, respectively.

Comparison results for Frankston sand

Donald (1956) conducted direct shear tests to measure unsaturated shear strength on well-graded Frankston sand. The Frankston sand specimens were prepared by the vibration technique to obtain the controlled medium dense sand. Once the specimen was prepared on the ceramic disk and set up in the apparatus, it was saturated allowing water, which was in the tank under atmospheric pressure conditions (zero pressure), to flow into the specimen through the ceramic disk. The saturation of the specimen was assumed to have occurred when the change in the mass of the water tank was negligible. At the same time, the normal stress was gradually increased to a predetermined value of 10 kPa.

Figure 7 demonstrates the comparison between predicted and measured results for Frankston sands. The suction of sands generally is quite low compared to clays. It is interesting to observe from experimental results that the unsaturated shear strength increases with increasing suction but begins to decrease when suction is continuously increased. Only the proposed model and the one of Vanapalli et al. (1996) is able to reflect reasonably this tendency while other
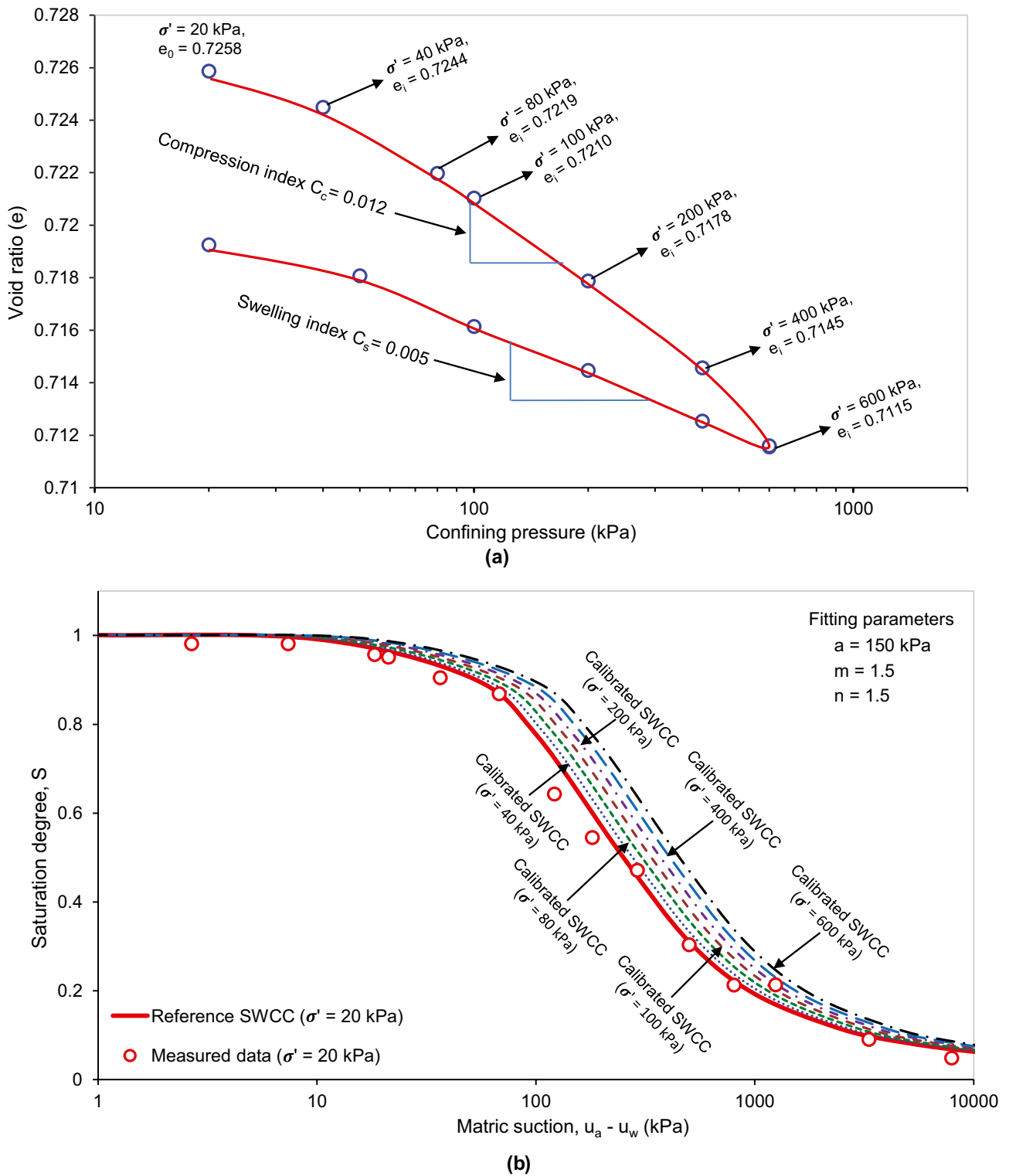
Fig. 4 Calibration procedure of SWCC (measured data source from Habasimbi and Nishimura [2019](#)): **a** compression curves of tested silt, **b** calibrated SWCC according to different confining pressure

models cannot consider this change. This is because both the proposed model and Vanapalli et al. ([1996](#)) model considered the suction contribution to the shear strength by using effective saturation degree. When suction is continuously increased over the residual value, the effective saturation degree becomes very small. As a result, the unsaturated
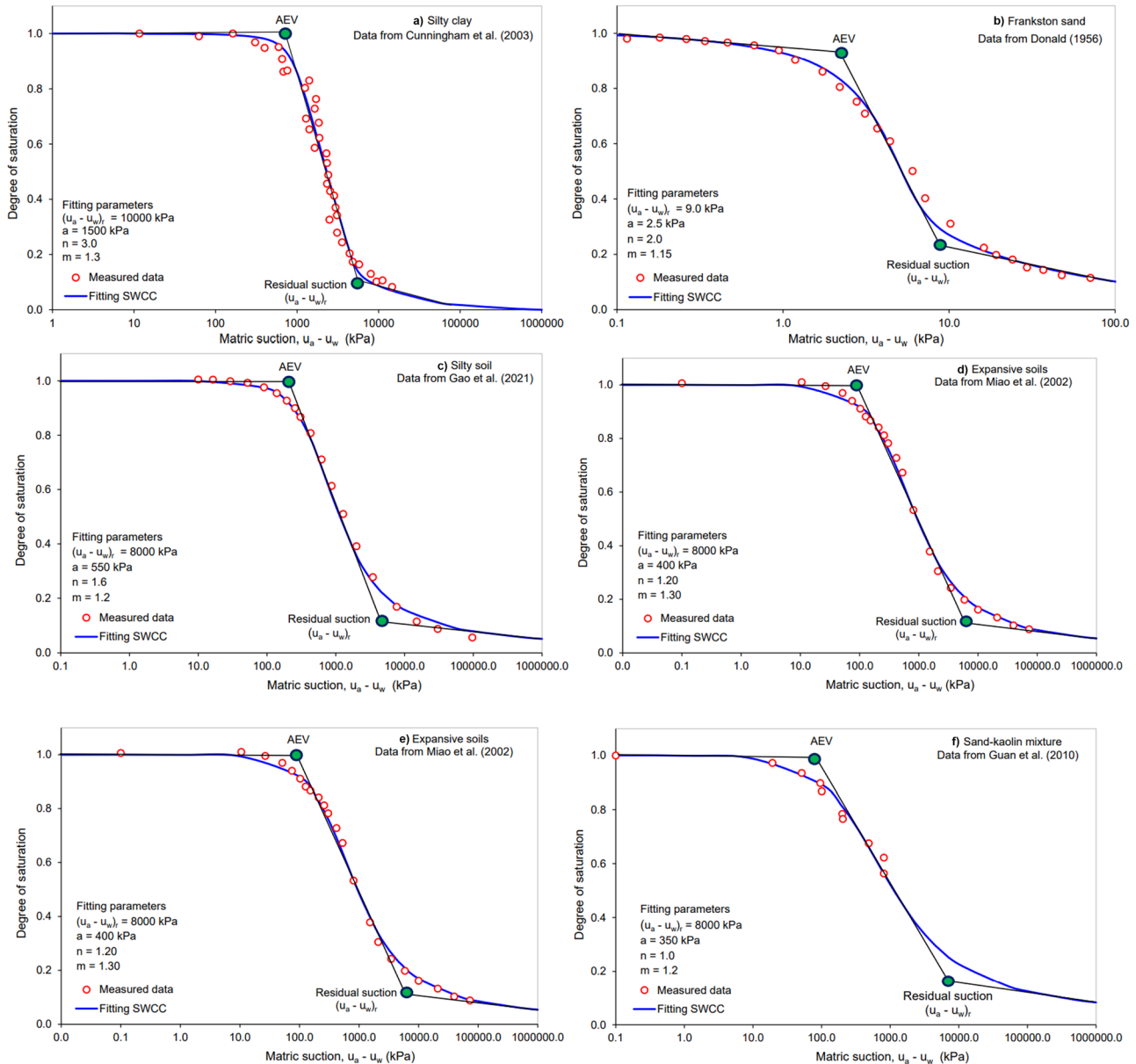
Fig. 5 Measured data and SWCCs of 6 different soil types

shear strength is reduced although suction increases. However, the proposed model gives a much better agreement with measured data compared to the model of Vanapalli et al. (1996). Value *ARE* was 1.2%, and 12% corresponding to the proposed model and model of Vanapalli et al. (1996). Additionally, it is found that the model of Khalili and Khabbaz (1998) only matches well with measured data for suction range lower than air-entry value but overpredicts considerably when suction is increased (*ARE* = 5.7%). It is also observed that the prediction performance of the Lamborn model (1986), and Naghadeh and Toker model (2019) is much lower than other models. The value *ARE* of these two models is 15.6% and 19.5%, respectively.

Comparison results for silty soils

Gao et al. (2021) conducted a series of suction-controlled triaxial compression tests on compacted silty soils. Silty clay specimens were prepared at the optimum water content (21%) and a dry density of 1.60 g/cm³. Firstly, the oven-dried kaolin powder and fine quartz sand with a ratio of 3:1 were mixed, and then, distilled water was added to produce the initial water content of 21%. The wet soil was then packed into a cylindrical mold in three layers of roughly equal thickness, and the static compaction method was used to achieve the necessary dry density. Finally, the soil specimen was gently removed from the mold once the compaction

Table 1 Characteristic of tested soils for comparison

Reference	Type of soils	Saturated shear strength parameter		Specific gravity G_s	Initial void ratio e_0	Initial water content w_s (%)	Air-entry value AEV (kPa)	Residual suction $(u_a - u_w)_r$	Residual saturation degree S_r
		Friction angle ϕ' (degree)	Effective cohesion c' (kPa)						
Cunningham et al. (2003)	Silty clays	32	0	2.64	0.51	20.5	1500	8000	0.1
Donald (1956)	Frankston sands	37	3.94	2.68	0.64	24.5	2.5	8.0	0.31
Gao et al. (2021)	Silty soils	21.8	54.4	2.63	0.66	21.0	550	8000	0.17
Kayadelen et al. (2007)	Residual clays	21.9	14.82	2.71	1.05	37.1	40	8000	0.14
Miao et al. (2002)	Expansive soils	21.3	32.0	2.70	0.83	17.0	25	1500	0.092
Guan et al. (2010)	Sand-kaolin mixture	26.9	8.5	2.67	0.51	19.0	41	8000	0.19

process was done. Before the triaxial tests, all specimens were saturated in a vacuum. The axis-translation technique is used to control the matric suction in these data sets. A saturated ceramic disc with a high air-entry value was used to apply pore air pressure to the top of the specimen, while a saturated ceramic disc with a high air-entry value was used to apply pore water pressure to the bottom.

A comparison between predicted and measured results for silty soils with the net normal stress of 100 kPa is shown in Fig. 8. It is observed that the results predicted the proposed model is in good agreement with measured data and generally better than other models, with the value *ARE* of only 1.2%. It is also interesting to note that three models of Vanapalli et al. (1996), Oberg and Sallfors (1997), Naghadeh and Toker (2019) produce a quite close prediction and agree relatively good with measured data. The value *ARE* for these three models is 2.1%, 2.3%, and 1.8% respectively. The low suction range combined with a high saturation degree can be considered an explanation for the small difference between the three models. It should also be noted that the model of Naghadeh and Toker (2019) is an empirical model that was established based on the test results of silt and the performance of this model seems to be better for silty soils than other soils. On the other side, it is also observed that the model of Lamborn (1986) produces a significant underprediction while the model of Khalili and Khabbaz (1998) gives a high overprediction. Value *ARE* of these two models are 19.6% and 14.2%, respectively.

Comparison results for clay

Kayadelen et al. (2007) investigated the influence of suction on the shear strength of soils using 12 unsaturated triaxial tests. By applying the axis translation technique, the matric suction in the soil specimen may be controlled. The soil samples were saturated prior to the experiments. Using the axis translation, a known magnitude of air pressure was delivered to soil specimens after the saturation process. The soil specimens were then desaturated by eliminating pore water before shearing, and a certain matric suction value was required.

Figure 9a presents the comparison between the proposed model and experimental data for a suction range of 0 to 400 kPa. It can be seen that the proposed model produces a good match to measured data for different suction values. The value *ARE* of the proposed model is only 4.65%. The proposed model is then compared with existing shear strength and measure data for net normal stress case of 50 kPa, and results are indicated in Fig. 9b. It is worthy to note that both analytical and experimental models agree that the shear strength increases nonlinearly with an increase in matric suction. However, the proposed model shows a prediction performance better than other models. The model of Naghadeh and Toker (2019) also produces a good prediction in this case with a value *ARE* of 7.2% while the value *ARE* was 11.3% for the Vanapalli et al. model (1996) and 12.9% for the model of Oberg and Sallfors (1997), whereas a low prediction performance is observed for the models of Lamborn (1986), Khalili and Khabbaz (1998), in which the value *ARE* of these two models is 22.8%, and 20.6%, respectively.

Comparison results for expansive soils

To determine the shear strength of unsaturated expansive soil, Miao et al. (2002) conducted a series of unsaturated triaxial experiments. The samples are remolded expansive soils that have been statically compacted to measure water

Fig. 6 Comparison outcomes for silty clay (measured data source from Cunningham et al. 2003): **a** proposed model against measured data, **b** performance comparison of shear strength models
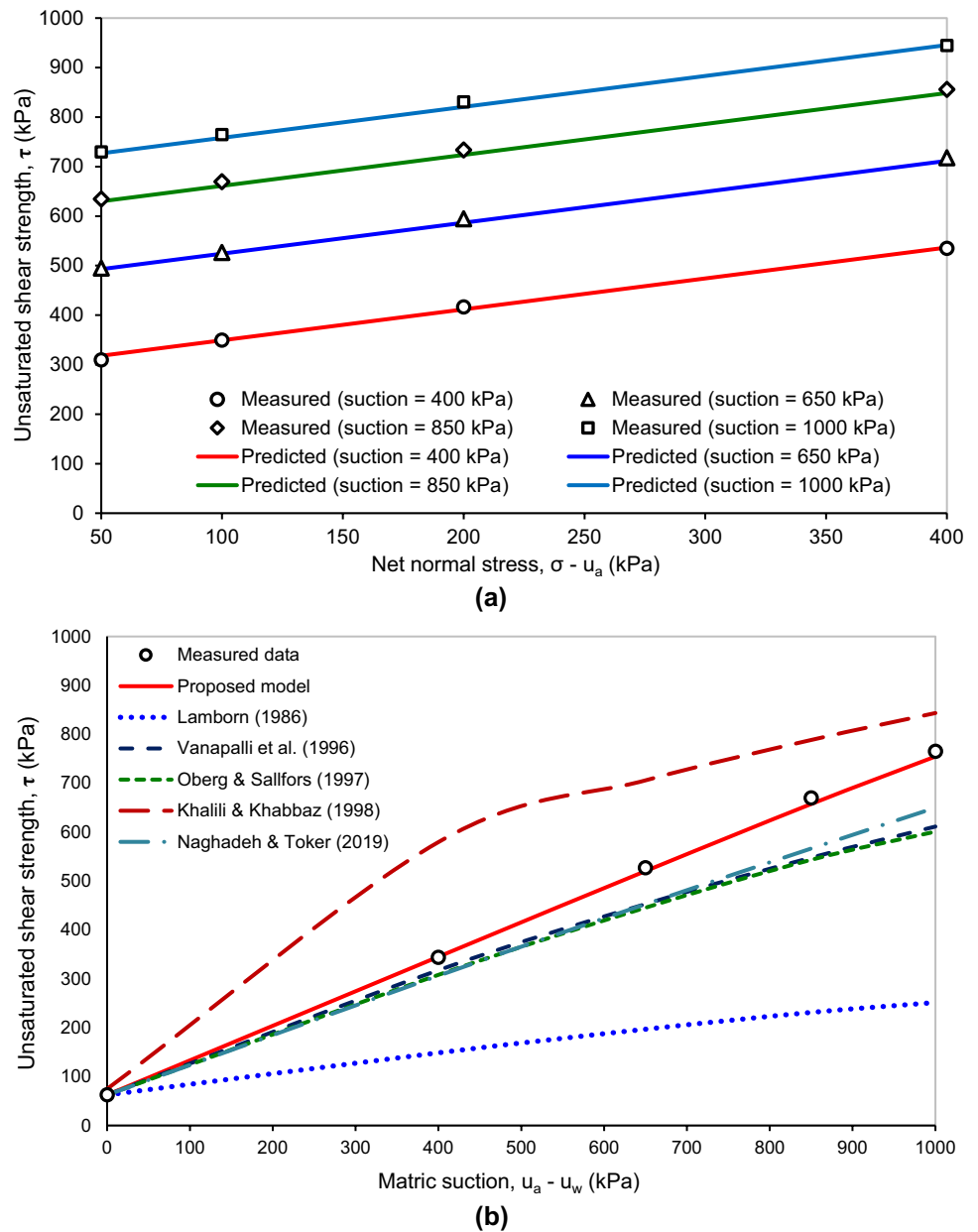
content and density condition. Controlling suction for four equivalent values: 50, 80, 120, and 200 kPa is used to assess unsaturated soils. The tests are conducted in a draining condition with a shear rate of 0.009 mm/min.

Figure 10a shows the comparison between the proposed model and measured data for expansive soils. It is relatively interesting to note that the proposed model agrees well with measured data for all different cases, where variation in matric suction and net normal stress occurs simultaneously. The value *ARE* of the proposed model, in this case, was only 0.8%. Comparison results between analytical and experimental models are presented in Fig. 10b. It is noted that the model of Khalili and Khabbaz (1998), and the one of Naghadeh and Toker (2019) produce a high overprediction

of unsaturated shear strength. The value *ARE* of the two models is 35% and 16%, respectively. On the other hand, the model of Lamborn (1986) highly underpredicts the shear strength of unsaturated soils, which is specialized by the value *ARE* of 26.2%. It is also observed that the prediction performance of models of Vanapalli et al. (1996), and Oberg and Sallfors (1997) decreases with increasing suction. The value *ARE* was 7.53% for the model of Vanapalli et al. (1996), and 8.33% for Oberg and Sallfors (1997).

Comparison results for sand-kaolin mixture

Guan et al. (2010) conducted a series of shear strength tests on the sand-kaolin mixture using modified triaxial apparatus.

Fig. 7 Comparison outcomes for Frankston sands (measured data source from Donald 1956)
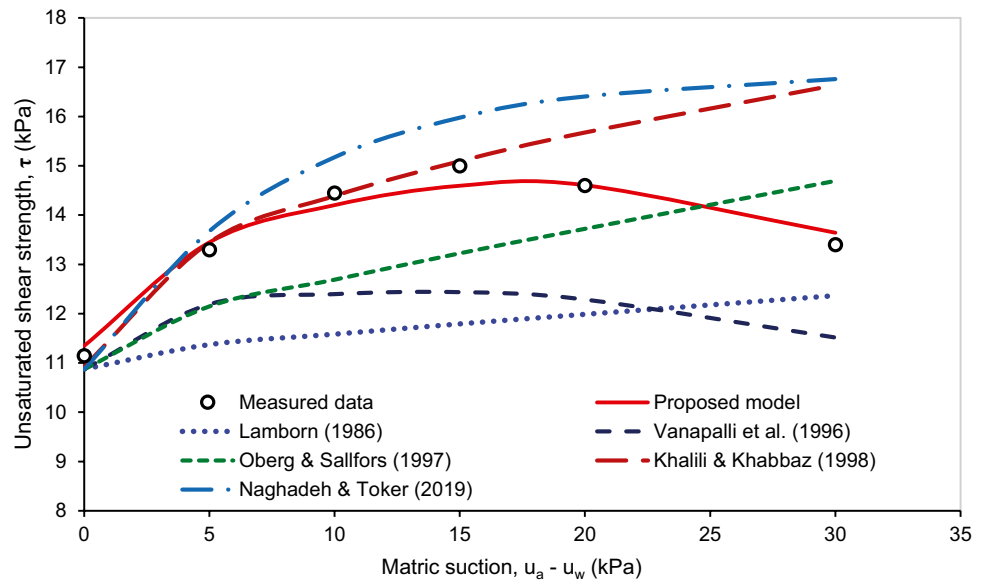
The sand-kaolin mixture comprises 35% of sand and 65% of kaolin. The sand-kaolin specimens were statically compacted to obtain the maximum dry density of 1.67 g/cm³ and the optimum water content of 19%. All specimens were saturated at the beginning of the test to have a uniform initial condition and to reduce the matric suction to a low value. Saturation was performed by applying cell pressure and back pressure from digital pressure and volume controller equipment. The specimen was then isotropically consolidated to the designated net confining pressure. Once consolidation was completed, the drying process of the specimen was conducted by applying the designated matric suction using the axis translation technique.

Figure 11 shows a comparison between predicted and measured results for the sand-kaolin mixture. Like other

soil types, it can be observed that the model of Khalili and Khabbaz (1998) produces a high overprediction while the model of Lamborn (1986) provides a significant underprediction of unsaturated shear strength. The value *ARE* of the two models was 19.3% and 25%, respectively. The models of Vanapalli et al. (1996), Oberg and Sallfors (1997), and Naghadeh and Toker (2019) also underpredict slightly the shear strength of unsaturated sand-kaolin mixture. The value *ARE* of the three models was 9.02%, 9.76%, and 5.82%, respectively. However, it should also be noted that the performance of these three estimation models tends to decrease with an increase in matric suction. It is observed that the proposed model gives a good agreement with measured data and is generally better than other models when the value *ARE* was only 2.1%.

Fig. 8 Comparison outcomes for silty soils (measured data source from Gao et al. 2021)
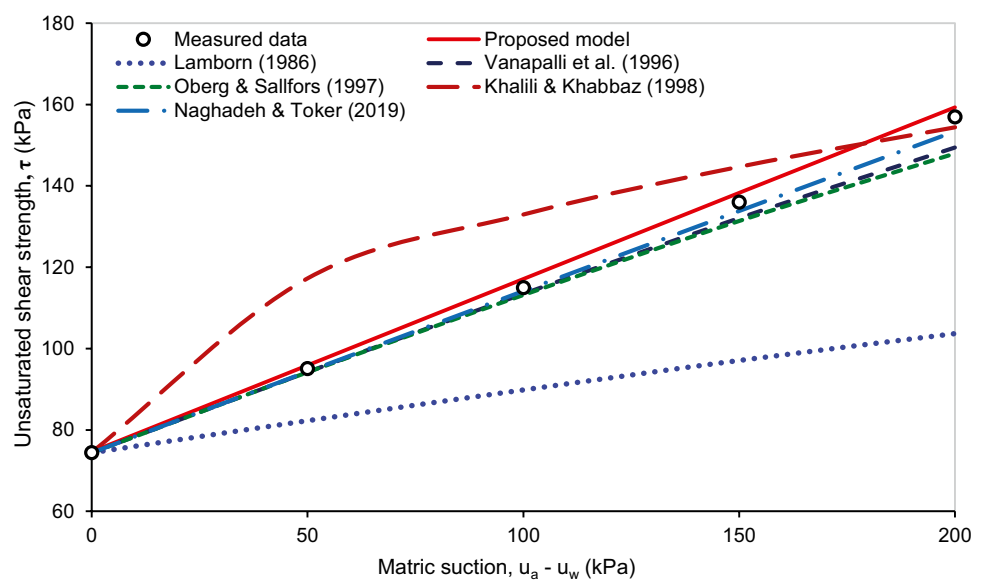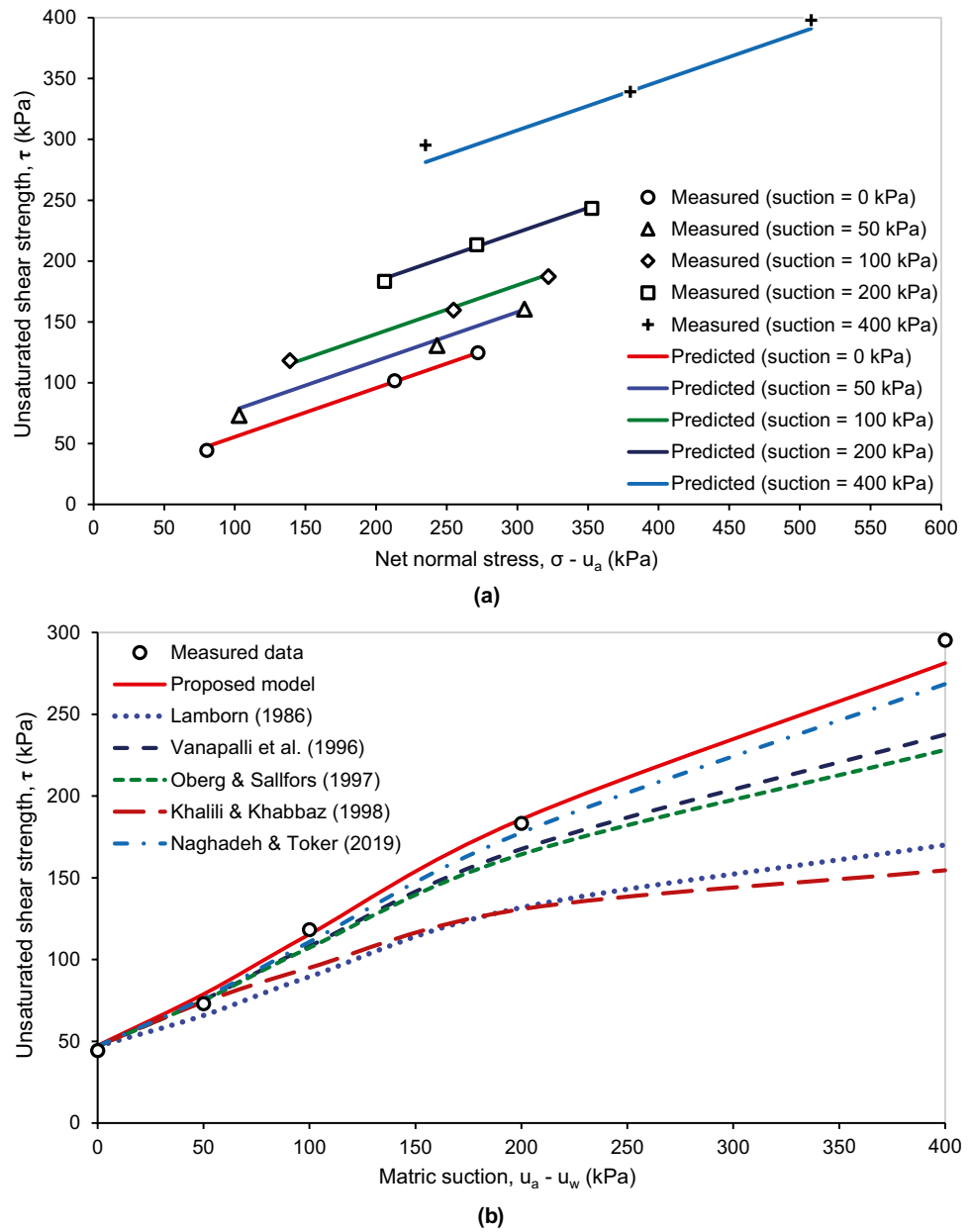
Fig. 9 Comparison outcomes for clays (measured data source from Kayadelen et al. 2007): **a** proposed model against measured data, **b** prediction performance of shear strength models


(a)

(b)

Statistical evaluation

A statistical evaluation was conducted on six different soil types for shear strength models, as shown in Fig. 12. It is interesting to note that the value *ARE* of the proposed model was less than 10% among all six cases which reveals that the proposed equation has a good and reliable performance in predicting the shear strength of unsaturated soils. It is also noted that the models of Lamborn (1986), Khalili and Khabbaz (1998) show a lower performance for different soil types, among the considered models. Definition of SPF based on volumetric water content or air-entry value can be considered the reason behind the lower performance. It should be noted that the prediction

performance of models of Vanapalli (1996), Oberg and Sallfors (1997), and Naghadeh and Toker (2019) is quite similar. However, the model of Vanapalli (1996), and the model of Naghadeh and Toker (2019) are much sensitive to the accuracy of residual value. Another interesting finding is that the prediction performance of shear strength models for the clayey soils and expansive soils is lower than that for silty and sandy soils.

The measured against predicted shear strength is presented in Fig. 13. The results indicate that the proposed model shows an excellent performance in estimating shear strength for any suction range. It is also found that the existing shear strength models tend to agree well with measured data for low shear strength range but differ significantly

Fig. 10 Comparison outcomes for expansive soils (measured data source from Miao et al. 2002): **a** proposed model against measured data, **b** prediction performance of shear strength models
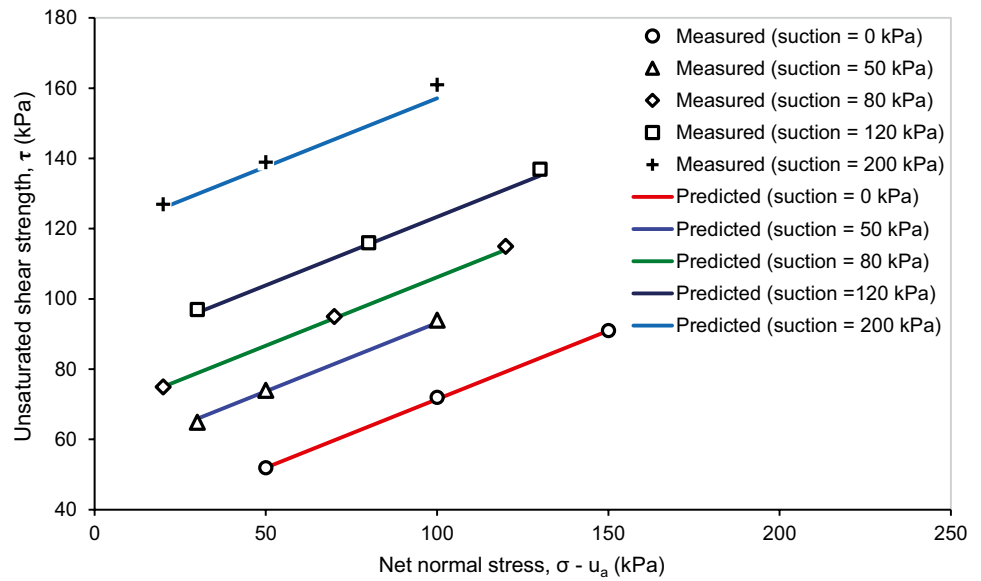

(a)
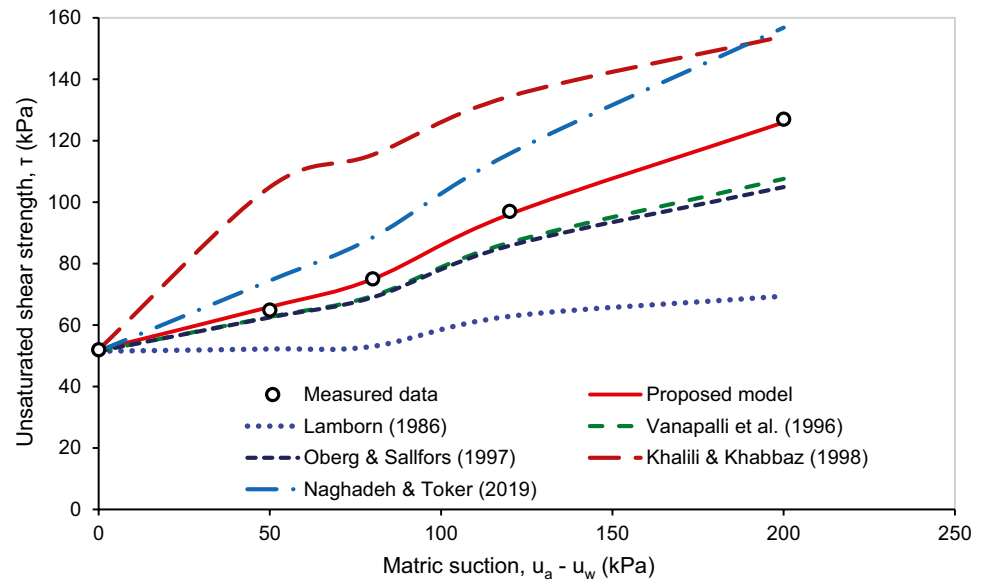
(b)

when the shear strength range is increased. It is interesting to note that the model defining SPF based on residual suction value (Naghadeh and Toker 2019) gives a better prediction than the one defining SPF based on air-entry value (Khalili and Khabbaz 1998).

Non-isothermal shear strength model for unsaturated soils

It is well known that climatic conditions subject soils near the ground surface to cyclic heating and cooling episodes. However, the shear strength characteristics of soils are highly affected by temperature variations. As temperature increases, the reduction of matric suction and void ratio triggers the change of shear strength. Therefore, it is a necessity to estimate the shear strength of soils with temperature change. As a result, the proposed model is further extended to predict the effect of temperature on the unsaturated shear strength of soils in this section. It should be noted that a temperature increase tends to induce a variation in the shear strength of soils through four components: friction angle, cohesion, disturbance function, and matric suction. For the analysis, the following notation will be used: a subscript T indicates the current temperature, and a subscript T_0 indicates the reference temperature. The

Fig. 11 Comparison outcomes for sand-kaolin mixture (measured data source from Guan et al. 2010)
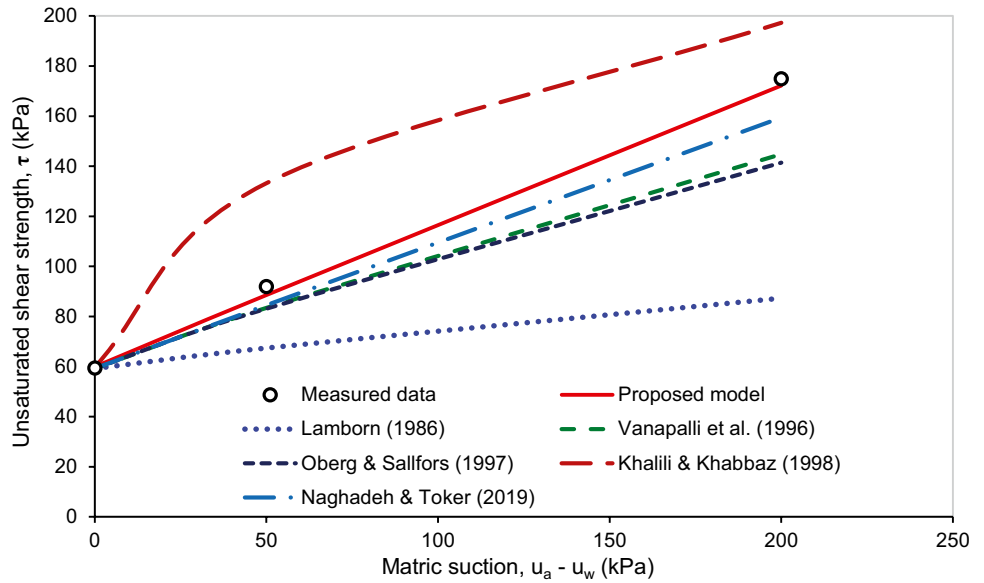
reference temperature is defined as the initial temperature of the soil sample during matric suction measurement in the laboratory and is often the same as room temperature.

Based on Eq. (28), the non-isothermal shear strength model for unsaturated soils can be expressed as follows:

$$\tau_T = c'_T + (\sigma - u_a) tan\, \varphi'_T + (u_a - u_w)_T \cdot \left[\theta_e + S_e \cdot (1 - \theta_e) \\ + D_T\right] tan\, \varphi'_T + u_w \cdot D_T \cdot tan\, \varphi'_T$$

(44)

where τ_T = unsaturated shear strength at temperature T, D_T is disturbance function at temperature T, $(u_a - u_w)_T$ is matric suction at temperature T, c'_T and φ'_T is cohesion and friction angle at temperature T. However, many researchers

found that the parameters c'_T and φ'_T are either independent of temperature change or the impact of temperature change is limited in most cases (Hueckel and Baldi 1990; Graham et al. 2001; Cekerevac and Laloui 2004; Laloui and Sutman 2021).

Temperature-dependent matric suction

In porous media, the mechanical and thermodynamic equilibrium is often derived from the relationship between capillary potential and the free energy of soil moisture (Arya and Paris 1981; Pham and Suman 2022). The matric suction or capillary pressure is determined by the following relation:

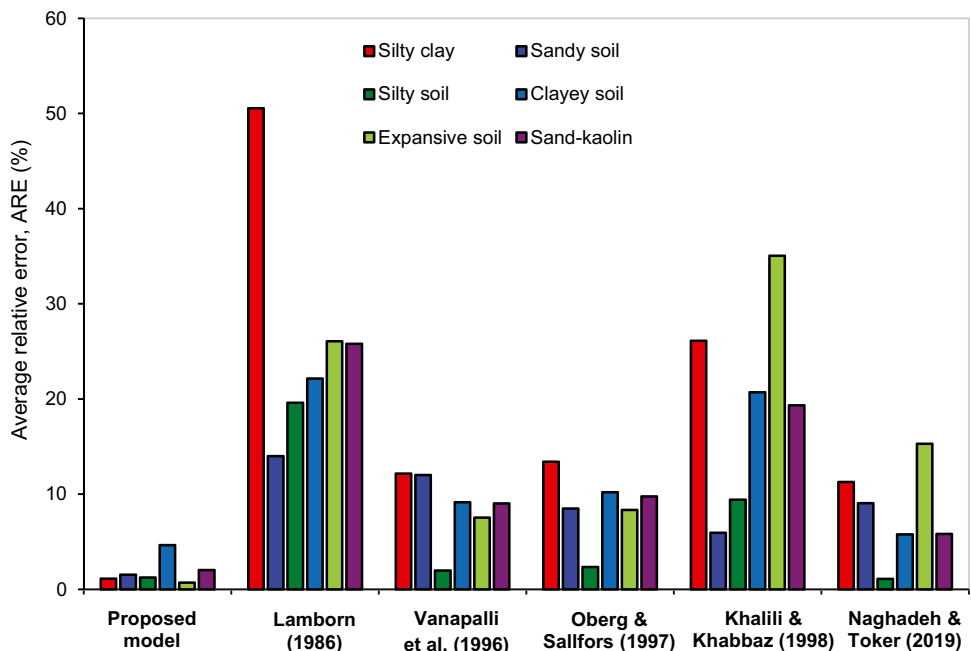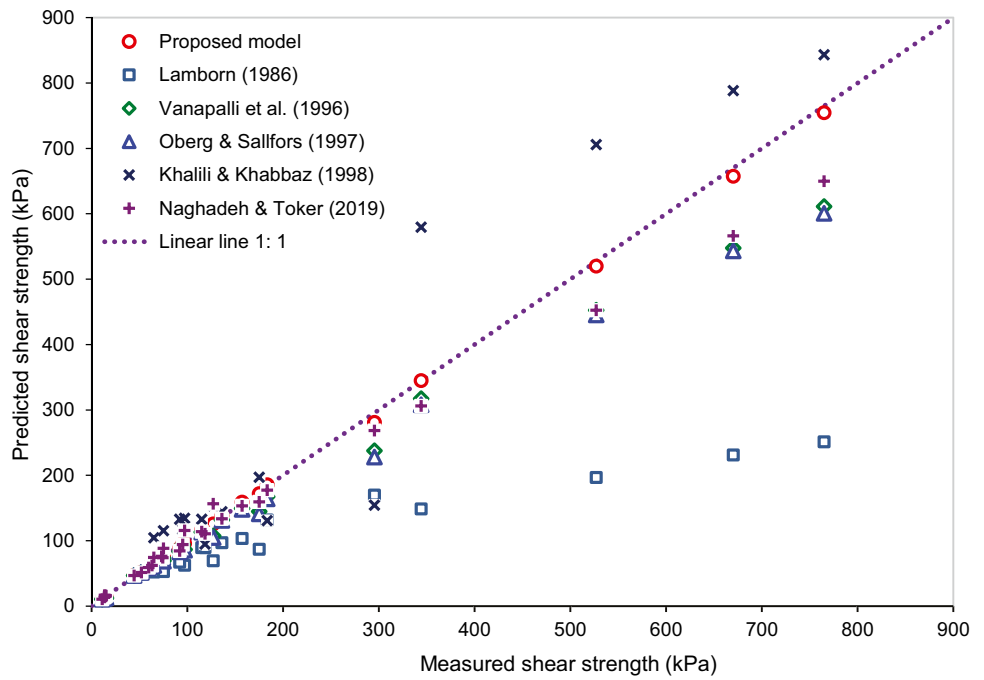**Fig. 12** Average relative error of models for different soil types

Fig. 13 Predicted versus measured shear strength

where σ_s is surface tension, $cos\alpha$ is contact angle, r_i is pore radius, R is particle radius, e is the void ratio, n_s is the number of particles for a soil volume, δ is a calibrated coefficient considering the real shape and orientation of soil particles.

The change of matric suction with temperature thus can be specialized through variation in surface tension, contact angle, particle radius, and void ratio as follows:

$$\psi = \frac{2\sigma_s \cdot cos\alpha}{r_i} = \frac{\sigma_s \cdot cos\alpha}{R \cdot \sqrt{e \cdot n_s^{1-\delta}/6}} \tag{45}$$

$$\frac{\partial(u_a - u_w)}{\partial T} = \frac{(u_a - u_w)}{\sigma_s} \cdot \frac{\partial \sigma_s}{\partial T} + \frac{(u_a - u_w)}{cos\,\alpha} \cdot \frac{\partial \cos\alpha}{\partial T} - \frac{(u_a - u_w)}{R} \cdot \frac{\partial R}{\partial T} - \frac{(u_a - u_w)}{e} \cdot \frac{\partial e}{\partial T} \tag{46}$$

The matric suction at the current temperature $(u_a - u_w)_T$ can be related to the reference matric suction $(u_a - u_w)_{T_0}$ by the simplified form as follows:

$$(u_a - u_w)_T = (u_a - u_w)_{T_0} \times f_\sigma \times f_\alpha \times f_R \times f_e \tag{47}$$

where

$$f_\sigma = \frac{\sigma_{sT}}{\sigma_{s0}} = \frac{96.76 - 0.0125 \times T - 0.000238 \times T^2}{96.76 - 0.0125 \times T_0 - 0.000238 \times T_0^2} \tag{48}$$

$$f_\alpha = \frac{cos\,\alpha_T}{cos\,\alpha_0}$$
$$= \frac{(96.76 - 0.0125 \times T - 0.000238 \times T^2) \cdot T_0}{(96.76 - 0.0125 \times T_0 - 0.000238 \times T_0^2) \cdot T + (0.000238 T^2 + 0.09676) \cdot (T - T_0)} \tag{49}$$

$$f_R = \frac{R_0}{R_T} = \frac{1}{\sqrt[3]{1 + \beta_v \cdot (T - T_0)}} \tag{50}$$

$$f_e = \sqrt{\frac{e_0}{e_T} \cdot \left(\frac{1 + e_T}{1 + e_0}\right)^\delta} \tag{51}$$

in which f_σ is the temperature-dependent function of surface tension, f_α is the temperature-dependent function of air–water contact angle, f_R is the temperature-dependent function of particle radius, f_e is the temperature-dependent function of void ratio, β_v is volumetric thermal expansion coefficient of solids, e_0 and e_T are initial void ratios at reference and current temperature respectively. It should be noted that T is expressed in degrees Kelvin (K) in the above formulae.

**Temperature-dependent disturbance function**

The disturbance function is known to depend on the void ratio of soils. The void ratio of soils generally varies with the temperature change. The disturbance function considering thermal volume change, therefore, can be re-written as follows:

$$D_T \approx D_0 \cdot \frac{(1 + e_0)^{2/3}}{(1 + e_T)^{2/3}} \tag{52}$$

where D_0 is the disturbance function at reference temperature (T_0).

Demars and Charles (1982) found that the void ratio variation of normally consolidated soils due to temperature

Fig. 14 Soil–water characteristic curve at different temperatures (measured data source from Uchaipichat and Khalili 2009)
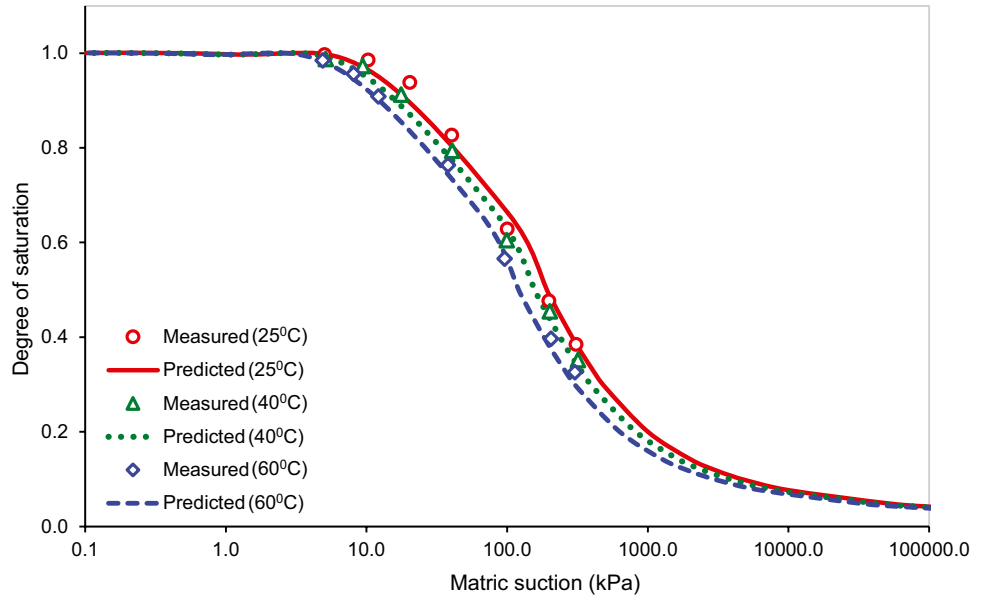
fluctuation is directly related to soil plasticity. Based on experimental outcomes, an equation that describes the relationship between change in void ratio due to temperature cycle and plasticity index is proposed as follows:

$$e_T = e_0 - \left(0.00048 + 0.0000088 I_P\right)\Delta T \tag{53}$$

where I_P is the index of plasticity, ΔT is temperature increment (°K).

Validation of non-isothermal shear strength model

The validation of the non-isothermal shear strength model is investigated against experimental results on the unsaturated compacted silt. Uchaipichat and Khalili (2009)

conducted a comprehensive program of non-isothermal testing on a compacted sample of silt in a modified triaxial cell. Applied temperature values ranged from 25 to 60 °C, and the suction values varied from 0 to 300 kPa. The soil was statically compacted to a dry unit weight of about 1.53 g/cm³, and at a moisture content of 10.5%. The samples were prepared dry of optimum to render the soil matrix amenable to stiffening with increasing matric suction. Before compaction, the soil was air-dried at room temperature, ground by a rubber hammer, and screened through a 400 µm sieve. Then, it was carefully wetted with a spray gun to a water content of 10.5% and placed in a sealed plastic bag to cure for 24 h for moisture equalization.

Fig. 15 Comparison between predicted and measured results at different temperatures
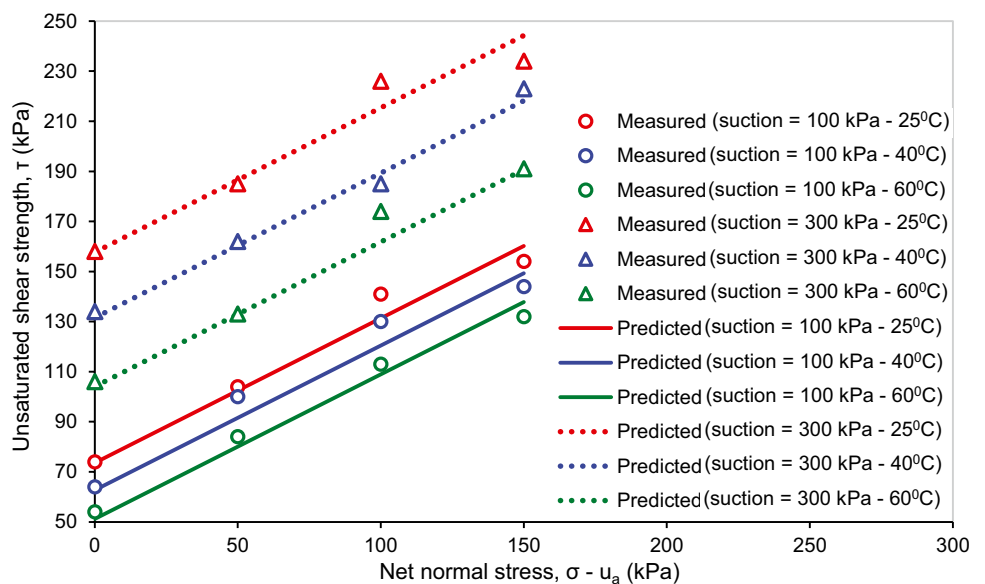
It should be noted that the variation in soil–water characteristic curve with temperature (non-isothermal SWCC) can be predicted by combining Eqs. (41) and (47) in this study. Figure 14 shows the comparison between predicted and measured results for the non-isothermal SWCC. It is observed that the predicted SWCC matches well with measured data for different values of temperature. Both analytical and experimental models agree that higher temperature produces lower SWCC, which corresponds to a reduction in suction with increasing temperature. However, the effect of temperature on SWCC is only significant for the suction range in the transition zone (between air-entry value and residual value).

Figure 15 presents comparison outcomes for unsaturated shear strength at elevated temperatures. It is interesting to note that the unsaturated shear strength decreases with increasing temperature. However, the influence degree of temperature on shear strength depends strongly on the suction range. For example, the unsaturated shear strength decreases 14.2% at the suction of 100 kPa and 18.6% at the suction of 300 kPa when the temperature is increased from 25 to 60 °C. It is also worthy to note that the value *ARE* was 4.2%, which indicates that the proposed model produces a high satisfaction with measured data for predicting the variation in shear strength with temperature.

Conclusions

In this paper, the evolution of the shear strength of unsaturated soils concerning the matric suction was studied under isothermal and non-isothermal conditions. Several main conclusions can be drawn from this study as follows:

A new shear strength equation based on the micromechanical model and the disturbed state concept was presented for unsaturated soils. The original point of this study is considering the solid contact area ratio which was neglected among most current models. Using the proposed model, the non-linear relationship between the matric suction, saturation degree, and the shear strength of unsaturated soils is described.

The results obtained from the proposed model were compared to several existing shear strength models and measured data for six different types of soils. The results indicate that the proposed model has a good performance in predicting the shear strength of unsaturated soils, and generally is better than other existing models. It is also found that the models defining SPF based on effective saturation degree give a better prediction than the models defining SPF based on the air-entry value or volumetric water content.

In response to varying climatic conditions, the proposed model was then extended to produce a non-isothermal shear strength equation for unsaturated soils. Validation of non-isothermal shear strength and SWCC models was performed against the experimental data on compacted silt. The comparison results show a good performance of the proposed model in predicting the shear strength variation with temperature.

Notation A: Total section area (m^2); A_c: Solid contact area between the two soil grains (m^2); A_w: Total water area (m^2); e: Void ratio (dimensionless); f: Water distribution function (dimensionless); f_σ: Temperature-dependent function of surface tension (dimensionless); f_α: Temperature-dependent function of air–water contact angle (dimensionless); f_r: Temperature-dependent function of particle radius (dimensionless); f_e: Temperature-dependent function of void ratio (dimensionless); σ: Total stress (Pa); σ_c: Solid contact stress (Pa); σ': Effective stress (Pa); c': Effective cohesion (Pa); c'_T: Cohesion at temperature T (Pa); c_i: Cohesion intercept (Pa); D_T: Disturbance function at temperature T; D: Disturbance function or solid contact area ratio (dimensionless); I_P: Index of plasticity (dimensionless); M: Slope of the critical state line (dimensionless); N: Total number of data points available; n: Porosity of soils (dimensionless); n_s: Number of contact points (dimensionless); P: Total external load applied on the unsaturated soil (N); P_c: Force transferred through the grain contact (N); P_w: Total force carried by pore water (N); P_a: Force carried by pore air (N); P_w^m: Forces carried by water in two menisci (N); p: Net mean stress (Pa); q: Deviatoric stress (Pa); u_w: Pore water pressure (Pa); u_a: Pore air pressure (Pa); $u_a - u_w$: Matric suction (Pa); $(u_a - u_w)_r$: Residual suction (Pa); $(u_a - u_w)_T$: Matric suction at temperature T (Pa); R: Particle radius (m); S_e: Effective saturation degree (dimensionless); S_r: Residual degree of saturation (dimensionless); T: Current temperature (Kelvin degree); t: Contact thickness (m); V_w^f: Free water volume (m^3); V_w^m: Menisci water volume (m^3); V_c: Total solid contact volume (m^3); V_{ci}: Contact volume between two solids (m^3); V_s: Solid volume (m^3); V_{si}: Volume of a solid particle (m^3); φ': Friction angle of soils at saturated condition (degree); φ'_T: Friction angle at temperature T (degree); $\tau_{measured}$: Measured shear strength value of ith data (Pa); $\tau_{predicted}$: Predicted value of shear strength of ith data (Pa); τ_T: Unsaturated shear strength at temperature T (Pa); α: Contact angle (radian); χ: Bishop's parameter (Pa); θ_e: Normalized volumetric water content (dimensionless); θ: Volumetric water content (dimensionless); θ_r: Volumetric water content at residual suction (dimensionless); θ_s: Volumetric water content at saturated

condition (dimensionless); β_v : Volumetric thermal expansion coefficient of solids (dimensionless)

Abbreviations DEM: Discrete element method; SWCC : Soil-water characteristic curve; AEV: Air-entry value; ARE: Average relative error; SPF: Soil property function

References

Abed AA, Vermeer PA (2009) Numerical simulation of unsaturated soil behaviour. Int J Comput Appl Technol 34(1):2–12. https://doi.org/10.1504/IJCAT.2009.022697

Alonso EE, Gens A, Josa A (1990) A constitutive model for partially saturated soils. Géotechnique 40(3):405–430. https://doi.org/10.1680/geot.1990.40.3.405

Alonso EE, Pereira JM, Vaunat J, Olivella S (2010) A microstructurally based effective stress for unsaturated soils. Géotechnique 60(12):913–925. https://doi.org/10.1680/geot.8.P.002

Arya LM, Paris JF (1981) A physicoempirical model to predict the soil moisture characteristic from particle-size distribution and bulk density data. Soil Sci Soc Am J 45(6):1023–1030. https://doi.org/10.2136/sssaj1981.03615995004500060004x

Aubeny C, Lytton R (2003) Estimating strength versus location and time in high-plasticity clays (No. FHWA/TX-03/2100-P1). Texas Transportation Institute, Austin, Texas, USA.

Bishop AW, Alpan I, Blight GE, Donald IB (1960) Factors controlling the shear strength of partly saturated cohesive soils. Proc 5th Intern Conf on Soil Mech Foundation Engineering, Paris, France 1:13–21

Blatz JA, Graham J (2003) Elastic-plastic modelling of unsaturated soil using results from a new triaxial test with controlled suction. Géotechnique 53(1):113–122. https://doi.org/10.1680/geot.2003.53.1.113

Cai G, He X, Dong L, Liu S, Xu Z, Zhao C, Sheng D (2020) The shear and tensile strength of unsaturated soils by a grain-scale investigation. Granular Matter 22(1):1. https://doi.org/10.1007/s10035-019-0969-4

Cekerevac C, Laloui L (2004) Experimental study of thermal effects on the mechanical behaviour of a clay. Int J Numer Anal Meth Geomech 28(3):209–228. https://doi.org/10.1002/nag.332

Cho SE, Lee SR (2001) Instability of unsaturated soil slopes due to infiltration. Comput Geotech 28(3):185–208. https://doi.org/10.1016/S0266-352X(00)00027-6

Cunningham MR, Ridley AM, Dineen K, Burland JB (2003) The mechanical behaviour of a reconstituted unsaturated silty clay. Géotechnique 53(2):183–194. https://doi.org/10.1680/geot.2003.53.2.183

Dastjerdi MT, Habibagahi G, Nikooee E (2014) Effect of confining stress on soil water retention curve and its impact on the shear

strength of unsaturated soils. Vadose Zone J. 13(5). https://doi.org/10.2136/vzj2013.05.0094

Demars KR, Charles RD (1982) Soil volume changes induced by temperature cycling. Can Geotech J 19(2):188–194. https://doi.org/10.1139/t82-021

Desai CS, Wang Z (2003) Disturbed state model for porous saturated materials. Int J Geomech 3(2):260–265. https://doi.org/10.1061/(ASCE)1532-3641(2003)3:2(260)

Donald IB (1956) Shear strength measurements in unsaturated noncohesive soils with negative pore pressures. In: Proceedings of the 2nd Australia–New Zealand Conf Soil Mech Found Eng. Christchurch, New Zealand. Technical Publications Ltd., Wellington, New Zealand, pp 200–204

Estabragh AR, Javadi AA (2008) Critical state for overconsolidated unsaturated silty soil. Can Geotech J 45(3):408–420. https://doi.org/10.1139/T07-105

Fredlund DG, Xing A (1994) Equations for the soil-water characteristic curve. Can Geotech J 31(4):521–532. https://doi.org/10.1139/t94-061

Fredlund DG, Morgenstern NR, Widger RA (1978) The shear strength of unsaturated soils. Can Geotech J 15(3):313–321. https://doi.org/10.1139/t78-029

Fredlund DG, Xing A, Fredlund MD, Barbour SL (1996) The relationship of the unsaturated soil shear strength to the soil-water characteristic curve. Can Geotech J 33(3):440–448. https://doi.org/10.1139/t96-065

Gao QF, Zeng L, Shi ZN, Zhang R (2021) Evolution of unsaturated shear strength and microstructure of a compacted silty clay on wetting paths. Int J Geomech 21(12):04021233. https://doi.org/10.1061/(ASCE)GM.1943-5622.0002207

Goh SG, Rahardjo H, Leong EC (2014) Shear strength of unsaturated soils under multiple drying-wetting cycles. J Geotech Geoenviron Eng 140(2):06013001. https://doi.org/10.1061/(ASCE)GT.1943-5606.0001032

Gong L, Nemcik J, Ren T (2018) Numerical simulation of the shear behavior of rock joints filled with unsaturated soil. Int J Geomech 18(9):04018112. https://doi.org/10.1061/(ASCE)GM.1943-5622.0001253

Graham J, Tanaka N, Crilly T, Alfaro M (2001) Modified Cam-Clay modelling of temperature effects in clays. Can Geotech J 38(3):608–621. https://doi.org/10.1139/t00-125

Guan GS, Rahardjo H, Choon LE (2010) Shear strength equations for unsaturated soil under drying and wetting. J Geotech Geoenviron Eng 136(4):594–606. https://doi.org/10.1061/(ASCE)GT.1943-5606.0000261

Habasimbi P, Nishimura T (2019) Soil water characteristic curve of an unsaturated soil under low matric suction ranges and different stress conditions. Int J Geosci 10(1):39–56. https://doi.org/10.4236/ijg.2019.101004

Hamid TB, Miller GA (2009) Shear strength of unsaturated soil interfaces. Can Geotech J 46(5):595–606. https://doi.org/10.1139/T09-002

Houston SL, Perez-Garcia N, Houston WN (2008) Shear strength and shear-induced volume change behavior of unsaturated soils from a triaxial test program. J Geotech Geoenviron Eng 134(11):1619–1632. https://doi.org/10.1061/(ASCE)1090-0241(2008)134:11(1619)

Hueckel T, Baldi G (1990) Thermoplasticity of saturated clays: experimental constitutive study. J Geotech Eng 116(12):1778–1796. https://doi.org/10.1061/(ASCE)0733-9410(1990)116:12(1778)

Jennings JEB, Burland JB (1962) Limitations to the use of effective stresses in partly saturated soils. Geotechnique 12(2):125–144. https://doi.org/10.1680/geot.1962.12.2.125

Jiang MJ, Leroueil S, Konrad JM (2004) Insight into shear strength functions of unsaturated granulates by DEM analyses. Comput

Geotech 31(6):473–489. https://doi.org/10.1016/j.compgeo.2004.07.001

Karube D, Kawai K (2001) The role of pore water in the mechanical behavior of unsaturated soils. Geotech Geol Eng 19(3):211–241. https://doi.org/10.1023/A:1013188200053

Kayadelen C, Tekinsoy MA, Taşkıran T (2007) Influence of matric suction on shear strength behavior of a residual clayey soil. Environ Geol 53(4):891. https://doi.org/10.1007/s00254-007-0701-2

Khaboushan EA, Emami H, Mosaddeghi MR, Astaraei AR (2018) Estimation of unsaturated shear strength parameters using easily-available soil properties. Soil Tillage Res 184:118–127. https://doi.org/10.1016/j.still.2018.07.006

Khalili N, Khabbaz MH (1998) A unique relationship for χ for the determination of the shear strength of unsaturated soils. Geotechnique 48(5):681–687. https://doi.org/10.1680/geot.1998.48.5.681

Kim H, Park SW (2020) DEM simulation for shear behavior in unsaturated granular materials at low-stress state. Comput Geotech 122:103551. https://doi.org/10.1016/j.compgeo.2020.103551

Kim J, Hwang W, Kim Y (2018) Effects of hysteresis on hydro-mechanical behavior of unsaturated soil. Eng Geol 245:1–9. https://doi.org/10.1016/j.enggeo.2018.08.004

Krisdani H, Rahardjo H, Leong EC (2008) Effects of different drying rates on shrinkage characteristics of a residual soil and soil mixtures. Eng Geol 102(1–2):31–37. https://doi.org/10.1016/j.enggeo.2008.07.003

Laloui L, Sutman M (2021) Experimental investigation of energy piles: From laboratory to field testing. Geomech Energy Environ 2:100214 https://doi.org/10.1016/j.gete.2020.100214

Lamborn MK (1986) A Micromechanic Approach to Modeling Partly Saturated Soils, Master of Science Thesis. Texas A&M University, College Station, Texas, USA

Lee IM, Sung SG, Cho GC (2005) Effect of stress state on the unsaturated shear strength of a weathered granite. Can Geotech J 42(2):624–631. https://doi.org/10.1139/t04-091

Lloret-Cabot M, Wheeler SJ, Sánchez M (2017) A unified mechanical and retention model for saturated and unsaturated soil behaviour. Acta Geotech 12(1):1–21. https://doi.org/10.1007/s11440-016-0497-x

Matsushi Y, Matsukura Y (2006) Cohesion of unsaturated residual soils as a function of volumetric water content. Bull Eng Geol Env 65(4):449. https://doi.org/10.1007/s10064-005-0035-9

Miao L, Liu S, Lai Y (2002) Research of soil–water characteristics and shear strength features of Nanyang expansive soil. Eng Geol 65(4):261–267. https://doi.org/10.1016/S0013-7952(01)00136-3

Mun BJ (2005) Unsaturated soil behavior under monotonic and cyclic stress states, Doctoral dissertation. Texas A&M University, Texas, USA

Naghadeh RA, Toker NK (2019) Exponential equation for predicting shear strength envelope of unsaturated soils. Int J Geomech 19(7):04019061. https://doi.org/10.1061/(ASCE)GM.1943-5622.0001435

Nam S, Gutierrez M, Diplas P, Petrie J (2011) Determination of the shear strength of unsaturated soils using the multistage direct shear test. Eng Geol 122(3–4):272–280. https://doi.org/10.1016/j.enggeo.2011.06.003

Niu G, Cui YJ, Pereira JM, Shao L, Sun D (2021) Determining Bishop's parameter χ based on pore size distribution. Géotech Lett 1–28 https://doi.org/10.1680/jgele.20.00095

Ng CW, Pang YW (2000) Influence of stress state on soil-water characteristics and slope stability. J Geotech Geoenviron Eng 126(2):157–166. https://doi.org/10.1061/(ASCE)1090-0241(2000)126:2(157)

Öberg AL, Sällfors G (1997) Determination of shear strength parameters of unsaturated silts and sands based on the water retention curve. Geotech Test J 20(1):40–48. https://doi.org/10.1520/GTJ11419J

Oh S, Lu N (2014) Uniqueness of the suction stress characteristic curve under different confining stress conditions. Vadose Zone J 13(5). https://doi.org/10.2136/vzj2013.04.0077

Patil UD, Hoyos LR, Puppala AJ (2016a) Modeling essential elastoplastic features of compacted silty sand via suction-controlled triaxial testing. Int J Geomech 16(6):D4016012. https://doi.org/10.1061/(ASCE)GM.1943-5622.0000726

Patil UD, Hoyos LR, Puppala AJ (2016b) Characterization of compacted silty sand using a double-walled triaxial cell with fully automated relative-humidity control. Geotech Test J 39(5):742–756. https://doi.org/10.1520/GTJ20150156

Patil UD, Puppala AJ, Hoyos LR, Pedarla A (2017) Modeling critical-state shear strength behavior of compacted silty sand via suction-controlled triaxial testing. Eng Geol 231:21–33. https://doi.org/10.1016/j.enggeo.2017.10.011

Pham TA (2022) Micromechanical-based shear strength equation considering the stress state effect for unsaturated soils. Int J Geomech (accepted).

Pham TA, Sutman M (2021) An analytical model for predicting the shear strength of unsaturated soils. Proc Inst Civ Eng: Geotech Eng 1–57 https://doi.org/10.1680/jgeen.21.00135

Pham TA, Sutman M (2022) Modeling the combined effect of initial density and temperature on the soil-water characteristic curve. Can Geotech J (under review).

Rassam DW, Cook F (2002) Predicting the shear strength envelope of unsaturated soils. Geotech Test J 25(2):215–220. https://doi.org/10.1520/GTJ11365J

Rojas E (2008) Equivalent stress equation for unsaturated soils. I: Equivalent stress. Int J Geomech 8(5):285–290. https://doi.org/10.1061/(ASCE)1532-3641(2008)8:5(285)

Romero E, Gens A, Lloret A (2001) Temperature effects on the hydraulic behaviour of an unsaturated clay. Geotech Geol Eng 19:311–332. https://doi.org/10.1023/A:1013133809333

Roy S, Rajesh S (2018) Influence of confining pressure on water retention characteristics of compacted soil. Indian Geotech J 48(2):327–341. https://doi.org/10.1007/s40098-017-0265-3

Satyanaga A, Rahardjo H (2019) Unsaturated shear strength of soil with bimodal soil-water characteristic curve. Géotechnique 69(9):828–832. https://doi.org/10.1680/jgeot.17.P.108

Schnellmann R, Rahardjo H, Schneider HR (2013) Unsaturated shear strength of a silty sand. Eng Geol 162:88–96. https://doi.org/10.1016/j.enggeo.2013.05.011

Tang CT, Borden RH, Gabr MA (2019) Model applicability for prediction of residual soil apparent cohesion. Transport Geotech 19:44–53. https://doi.org/10.1016/j.trgeo.2019.01.003

Tarantino A (2007) A possible critical state framework for unsaturated compacted soils. Géotechnique 57(4):385–389. https://doi.org/10.1680/geot.2007.57.4.385

Tarantino A, Tombolato S (2005) Coupling of hydraulic and mechanical behaviour in unsaturated compacted clay. Géotechnique 55(4):307–317. https://doi.org/10.1680/geot.2005.55.4.307

Toll DG (1990) A framework for unsaturated soil behaviour. Géotechnique 40(1):31–44. https://doi.org/10.1680/geot.1990.40.1.31

Uchaipichat A, Khalili N (2009) Experimental investigation of thermo-hydro-mechanical behaviour of an unsaturated silt. Géotechnique 59(4):339–353. https://doi.org/10.1680/geot.2009.59.4.339

Vanapalli SK, Fredlund DG (2000) Comparison of different procedures to predict unsaturated soil shear strength. Adv Unsaturated Geotech (pp. 195–209) https://doi.org/10.1061/40510(287)13

Vanapalli SK, Fredlund DG, Pufahl DE, Clifton AW (1996) Model for the prediction of shear strength with respect to soil suction. Can Geotech J 33(3):379–392. https://doi.org/10.1139/t96-060

Wang Q, Pufahl DE, Fredlund DG (2002) A study of critical state on an unsaturated silty soil. Can Geotech J 39(1):213–218. https://doi.org/10.1139/t01-086

Wheeler SJ, Sivakumar V (1995) An elasto-plastic critical state framework for unsaturated soil. Géotechnique 45(1):35–53. https://doi.org/10.1680/geot.1995.45.1.35

Ye W, Zhang Y, Chen B, Zhou X, Xie Q (2010) Shear strength of an unsaturated weakly expansive soil. J Rock Mech Geotech Eng 2(2):155–161. https://doi.org/10.3724/SP.J.1235.2010.00155

Zhai Q, Rahardjo H, Satyanaga A, Dai G (2019) Estimation of unsaturated shear strength from soil–water characteristic curve. Acta Geotech 14(6):1977–1990. https://doi.org/10.1007/s11440-019-00785-y

Zhai Q, Rahardjo H, Satyanaga A, Dai G, Zhuang Y (2020) Framework to estimate the soil-water characteristic curve for soils with different void ratios. Bull Eng Geol Env 79(8):4399–4409. https://doi.org/10.1007/s10064-020-01825-8

Zheng G, Shao L, Guo X, Zhang J (2020) Investigation of the mechanical behaviour of an unsaturated soil mixture using a digital image measurement system. Eur J Environ Civ Eng 24(8):1051–1067. https://doi.org/10.1080/19648189.2018.1442258